Long-term trends in seasonality and abundance of three key zooplankters in the upper San Francisco Estuary

Samuel M. Bashevkin[1*], Christina E. Burdi[2], Rosemary Hartman[3], Arthur Barros[2]

[1] Delta Science Program, Delta Stewardship Council, Sacramento, California, United States of America.

[2] California Department of Fish and Wildlife, Stockton, California, United States of America

[3] California Department of Water Resources, West Sacramento, California, United States of America

*Corresponding author: sam.bashevkin@waterboards.ca.gov

Acknowledgments

This work was conducted under the auspices of the Interagency Ecological Program (IEP). Funding for the IEP work plan element (062) CDFW Quantitative Analysis of Stomach Contents and Body Weight for Pelagic Fishes ("Diet and Condition Study") that collected the diet data was provided by contracts with the Department of Water Resources (R1730002) and the US Bureau of Reclamation (R20AC00089). The authors would like to thank Laurel Larsen, Steve Slater, Wim Kimmerer, David Senn, and an anonymous reviewer for comments on this manuscript and the field and laboratory staff of the Stockton CDFW office, particularly Tricia Bippus, Phillip Poirier, and Tom Gabel, for their tireless work in collecting and processing zooplankton and fish diet samples.

Abstract (300 words)

Zooplankton provide critical food for threatened and endangered fish species in the San Francisco Estuary (estuary). Reduced food supply has been implicated in the Pelagic Organism Decline of the early 2000s and further changes in zooplankton abundance,

seasonality, and distribution may continue to threaten declining fishes. While we have a wealth of monitoring data, we know little about the abundance trends of many estuary zooplankton species. To fill these gaps, we reviewed past research and then examined trends in seasonality and abundance from 1972 to present of three key but understudied zooplankton species (*Bosmina longirostris*, *Acanthocyclops* spp., and *Acartiella sinensis*) that play important roles in the estuary food web. We fit Bayesian generalized additive mixed models of each taxon's relationship with salinity, seasonality, year, and geography on an integrated database of zooplankton monitoring in the upper estuary. We found marked changes in the seasonality and overall abundance of each study species. *Bosmina longirostris* no longer peaks in abundance in the fall months, *Acanthocyclops* spp. dramatically declined in all months and lost its strong relationship with salinity, and *A. sinensis* adult abundance has become more strongly related to salinity while juveniles have developed wider seasonal abundance peaks. Through these analyses, we have documented the relationship of each species with salinity and seasonality since the beginning of monitoring or their introduction, thus increasing our understanding of their ecology and importance in the estuary. These results can inform food web models, be paired with fish data to model the contributions of these species toward fish abundance trends, and be mirrored to elucidate other species' trends in future studies.

Keywords

Zooplankton, phenology, salinity, monitoring, generalized additive modeling, copepods, cladocerans, *Bosmina longirostris*, *Acanthocyclops*, *Acartiella sinensis*

Introduction

Zooplankton are critical components of aquatic food webs, connecting primary producers to upper trophic species such as fishes. Most fishes rely on zooplankton as a food source during their larval stages when the starvation risk is highest (Hunter 1981). The

seasonality of fish reproduction is often timed such that larvae coincide with peaks in the abundance of their zooplankton prey (Cushing 1969; Cushing 1990). However, when the seasonality of zooplankton abundance or community composition shifts due to climate change, species introductions, or other factors, larval fish starvation risk can increase as their peak abundance no longer coincides with peak food availability (Edwards and Richardson 2004; Durant et al. 2007). Thus, an understanding of the patterns in zooplankton abundance is critical to understanding the drivers of fish abundance.

The San Francisco Estuary (estuary) is home to several fish species listed under the United States Endangered Species Act and/or the California Endangered Species Act. Most depend on zooplankton prey for part or all of their life cycle. One of these species, Delta Smelt (*Hypomesus transpacificus)* is endemic to the estuary and relies on zooplankton for its full life cycle (Brown et al. 2016). Another fish, Longfin Smelt (*Spirinchus thaleichthys*), also relies on zooplankton throughout its life cycle (Chigbu and Sibley 1998a; Chigbu and Sibley 1998b; Barros et al. 2022; Lojkovic Burris et al. 2022). A number of fish species, including Delta Smelt and Longfin Smelt, declined sharply in abundance in the early 2000s, during the "pelagic organism decline" (Feyrer et al. 2007; Sommer et al. 2007). This decline is thought to have been caused in part by reduced zooplankton food supply (Winder and Jassby 2011; Brown et al. 2016; Moyle et al. 2016).

Zooplankton research in the estuary to date has focused on a few key taxa, most notably the copepods *Pseudodiaptomus forbesi*, *Eurytemora affinis*, and *Limnoithona tetraspina*, as they are important food for threatened Delta Smelt and Longfin Smelt (Bouley and Kimmerer 2006; Kimmerer et al. 2014; Kayfetz and Kimmerer 2017; Kimmerer et al. 2018). In floodplains adjacent to the Delta, some cladocerans have also received attention, particularly *Daphnia* spp., due to their importance in the diet of juvenile salmonids (Goertler et al. 2018; Corline et al. 2021).

Many members of the zooplankton community remain understudied, despite their role in the pelagic food web. One prior study has investigated changes in zooplankton phenology in the estuary. Merz et al. (2016) used a high-level approach to evaluate changes (from 1972-2014) to the date of maximum abundance of five zooplankton taxa: *E. affinis*, *Pseudodiaptomus* spp., other calanoids, cyclopoids, and non-copepods. They found that the peak abundances of all these zooplankton groups except the cyclopoids have shifted weeks to months earlier. However, analyses of only the date of peak abundance can overlook the presence of multiple seasonal abundance peaks. Furthermore, the coarse taxonomic resolution of this study excluded analyses of some key species.

In this study, we extensively review prior knowledge and derive new insights from monitoring data in the estuary on three key but understudied zooplankton taxa. We chose to focus on *Bosmina longirostris*, *Acanthocyclops* spp., and *Acartiella sinensis* (Fig. 1) due to their importance in estuarine ecology and fish diets (Appendix A) as well as the paucity of prior studies on their dynamics in this estuary. For each taxon, we first review past studies from this estuary and other systems where these taxa occur, then ask 3 main questions to fill the remaining knowledge gaps: 1) What is the seasonal abundance pattern? 2) What is the relationship of abundance with salinity? and 3) How have long-term abundance, seasonal abundance patterns, and salinity relationships changed over time? To answer these questions, we apply Bayesian generalized additive mixed models to an integrated database of zooplankton monitoring data (Bashevkin et al. 2020; Bashevkin et al. 2022).

Background

Study area

The San Francisco Estuary (Fig. 2) is composed of the tidal, primarily freshwater Sacramento–San Joaquin Delta (Delta), which flows into brackish Suisun Bay, and then into the more saline San Francisco Bay. This study includes the Delta through the northernmost

99 embayment of San Francisco Bay (San Pablo Bay), since these are the areas with consistent
100 zooplankton monitoring data (hereafter referred to collectively as the upper estuary). The low
101 salinity zone is an important habitat feature defined by a range of salinities from 0.5-2 at the
102 low end up to 5-6 at the high end. It is an important nursery habitat for fishes such as Delta
103 and Longfin Smelt and moves geographically depending on outflow levels (and thus
104 seasonally – with higher outflow in winter and spring and lower outflow in summer and fall),
105 ranging between the Carquinez Strait westward and the lower Sacramento and San Joaquin
106 Rivers eastward (Hobbs et al. 2006). The Delta receives inflows primarily from the
107 Sacramento River to the north (85%) and the San Joaquin River to the south (11%), with
108 lesser inputs from eastern tributaries, the Cosumnes and Mokelumne Rivers (Kimmerer
109 2002). Almost all inflows come from reservoir releases since very few tributaries are left
110 undammed (Kimmerer 2004; Brown and Bauer 2010). Large export pumps in the South Delta
111 send a portion of these inflows to central and southern California. While annual total inflow
112 and outflow have not changed since the 1950s, inflows have shifted seasonally as reservoir
113 storage has increased in the spring and water releases have increased in the summer
114 (Kimmerer 2002; Hutton et al. 2017).

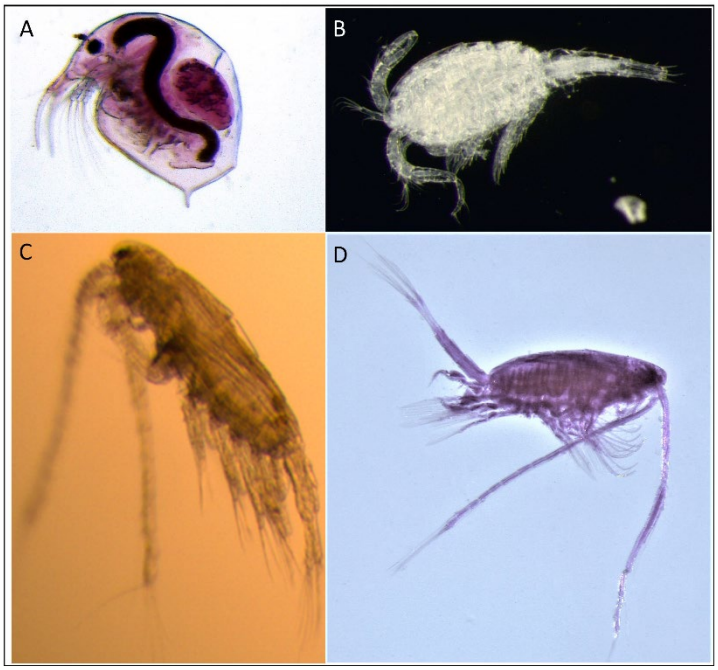

Figure 1. Photographs (not to scale) of our study species from the San Francisco Estuary. A) *Bosmina longirostris* adult (approximately 0.3 mm length, credit: CDFW Fish Restoration Program), B) *Acanthocyclops* spp. adult (approximately 1.1 mm length, credit: Tricia Bippus/CDFW), C) *Acartiella sinensis* juvenile male (approximately 1.1 mm length, credit: Anne Slaughter, Estuary & Ocean Science Center, San Francisco State University), D) *Acartiella sinensis* adult male (approximately 1.3 mm length, credit: Michelle Avila/CDFW Fish Restoration Program).

Prior research on the study species

Bosmina longirostris

Bosmina longirostris (Fig. 1A) is the most abundant cladoceran in the freshwater reaches of the Sacramento San Joaquin Delta (Bashevkin et al. 2020; Jeffres et al. 2020), where it has been a major component of the zooplankton community over the past 40 years (Ambler et al. 1985). Like *Daphnia* spp., it is abundant in off-channel habitat in the estuary (Corline et al. 2021), but unlike *Daphnia* spp., it is also abundant in the larger channels of the South Delta (Bashevkin et al. 2020; Jeffres et al. 2020). *Bosmina* spp. are consumed by fish including juvenile salmonids and juvenile and adult Delta Smelt (Appendix A) (Roegner et al. 2015; Goertler et al. 2018; Slater et al. 2019), but they rarely occur in the diets of larval

Longfin Smelt (Appendix A) (Jungbluth et al. 2021; Lojkovic Burris et al. 2022), likely due to a mismatch in the optimal salinities of *Bosmina* spp. and Longfin Smelt. Their small size makes them generally less consumed than larger *Daphnia* spp. by juvenile salmon (Craddock et al. 1976; Holm and Møller 1984), and juvenile perch with diets containing high percentages of *Bosmina* spp. result in low growth rates in a Swedish lake (Romare 2000). Both *Daphnia* spp. and *Bosmina* spp. tend to have lower nutritional quality (as measured by fatty acids) than copepods (Kratina and Winder 2015).

Bosmina longirostris is a small, filter-feeding cladoceran found in lakes and rivers throughout the world. Despite its widespread occurrence, its ecology has received little attention due to its small body size and complicated taxonomy (Adamczuk 2016). Despite its small size in comparison to members of the better-studied genus *Daphnia*, *B. longirostris* can still impact the food web. *Bosmina longirostris* is particularly effective in depressing biomass of small phytoplankton (Carpenter and Kitchell 1984) and is an efficient consumer of ciliates and bacteria (Jürgens et al. 1996), playing a key role in the microbial loop. *Bosmina longirostris* feeds broadly on phytoplankton, protists, and bacteria, ranging from 1-15 μm, and consumes algae rather than bacteria, when available (Balcer et al. 1984; Onandia et al. 2015). It can also thrive on many types of cyanobacteria (Tõnno et al. 2016). *Bosmina longirostris* is more tolerant of disturbance than many species of *Daphnia* (Hart 2004; Adamczuk 2016), with greater resistance to toxic cyanobacteria (Matveev and Balseiro 1990; Jiang et al. 2013; Jiang et al. 2014; Jiang et al. 2017), and a higher salinity tolerance than many other cladocerans (Adamczuk 2016). *Bosmina* spp. also have a higher thermal tolerance than many freshwater zooplankton (Drenner et al. 1981; Jiang et al. 2014), leading to the potential for their increasing advantage over other zooplankton as temperatures rise. *Bosmina longirostris* typically lives 20-50 days and reproduces parthenogenically, producing 2-6

broods of 2-4 embryos each, though temperature, salinity, and predation pressure may impact life span and reproduction (Adamczuk and Mieczan 2019).

Acanthocyclops spp.

Acanthocyclops spp. (Fig. 1B) is a cyclopoid of unknown origin which occurs mostly in freshwater (Orsi and Mecum 1986). Previous studies in the estuary identified the species of *Acanthocyclops* in this region as *Acanthocyclops vernalis;* however, research in other systems discovered that *A. vernalis* is a species complex consisting of three cryptic species; *Acanthocyclops robustus*, *Acanthocyclops americanus*, and *A. vernalis* (Alekseev et al. 2002; Dodson et al. 2003; Miracle et al. 2013; Alekseev 2021). Due to the potential for morphological misidentifications, it is not known whether all three species in the *A. vernalis* complex are native to the estuary or introduced at some point in the past; however, Jungbluth et al. (2021) did find molecular evidence of all these species in larval Longfin Smelt diets collected in this region in 2017.

Before the introduction of the small cyclopoid *L. tetraspina* in 1993 (Orsi and Ohtsuka 1999), *Acanthocyclops* spp. was the most abundant cyclopoid in the estuary (Orsi and Mecum 1986). *Acanthocyclops* spp. is an important component of fish diets in this region, particularly for Longfin Smelt (Appendix A) (CDFW unpublished data; Hobbs et al. 2006; Lojkovic Burris et al. 2022) and larval Pacific Herring (*Clupea pallasii*) (Jungbluth et al. 2021), with *Acanthocyclops* spp. being the most abundant cyclopoid detected in larval Longfin Smelt gut contents by molecular sequencing (Jungbluth et al. 2021). *Acanthocyclops* spp. also has a higher nutritional value than *L. tetraspina*, and a similar fatty acid composition to that of the calanoid copepods *E. affinis* and *P. forbesi* (Kratina and Winder 2015).

While research on the ecology and biology of *Acanthocyclops* spp. is relatively limited in the estuary, the *A. vernalis* complex has been studied extensively in other

freshwater and estuarine systems in Europe, Russia, and the Great Lakes. Studies in these systems show that, despite the morphological similarities, *A. vernalis*, *A. robustus*, and *A. americanus* have different ecologies, life cycles, and environmental tolerances (Alekseev et al. 2002; Miracle et al. 2013; Alekseev 2021). *Acanthocyclops vernalis* and *A. robustus* inhabit freshwater littoral or near-benthic areas and *A. vernalis* has a benthic naupliar stage (Alekseev et al. 2002; Miracle et al. 2013). Adult and juvenile *A. vernalis* also were found to vertically migrate from the bottom into the water column at night (Evans and Stewart 1977). Both *A. vernalis* and *A. robustus* are predominantly predatory, consuming copepod nauplii, cladocerans, rotifers, and occasionally larval fish (Anderson 1970; Kerfoot 1978; Gliwicz and Stibor 1993; Piasecki 2000). By contrast, *A. americanus* is pelagic throughout its lifecycle, has been found in salinities from the Mediterranean Sea (Alekseev 2021) to freshwater lakes (Alekseev et al. 2002), and is omnivorous. *Acanthocyclops americanus* nauplii consume primarily algae, with later life stages also consuming filamentous algae and cyanobacteria, in addition to cladocerans, nauplii, and rotifers (Enríquez-García et al. 2013; Sarma et al. 2019). All species can produce about 100 eggs per female, develop to sexual maturity in 10-14 days, and live 30-75 days depending on conditions, with *A. americanus* growing and reaching maturity faster than the other species (Alekseev 2021). Species in the *A. vernalis* complex likely have different environmental tolerances, as has been shown by studies of their seasonal and spatial variation in abundance in other regions. *Acanthocyclops vernalis* may be more tolerant of colder temperatures than the other species, whereas *A. americanus* could be tolerant of higher temperatures based on laboratory experiments and timing of peak abundance in areas outside the estuary (Alekseev 2021).

Acartiella sinensis

In the fall of 1993, the non-native calanoid copepod *A. sinensis* (Fig. 1C, D) was first detected in the estuary (Orsi and Ohtsuka 1999). Likely introduced via the ballast water of

ships, the large (~1.2 – 1.5 mm in length) predatory calanoid is native to Southeast Asia (Shen and Lee 1963; Srinui and Ohtsuka 2015). The species has been recorded from estuaries along the East China Sea in salinities around 18-21 (Shen and Lee 1963) to the brackish marshes of Thailand in salinities around 5 and average water temperatures around 31 ºC (Srinui and Ohtsuka 2015). In the Pearl River estuary of China, *A. sinensis* was the dominant copepod in brackish waters with salinities less than 15 (Tan et al. 2004). Sampling in the Thale-Noi lake of Thailand showed changes in temperature and salinity were the main environmental variables impacting densities of *A. sinensis* in the region (Inpang 2008).

Within a year after introduction, *A. sinensis* became the second most common calanoid copepod in the upper estuary, with its highest abundances in the low salinity zone during summer and fall (Hennessy 2018). *Acartiella sinensis* is predatory and has been shown to feed on copepod nauplii and copepodids, primarily *L. tetraspina* and *P. forbesi* (York et al. 2014; Slaughter et al. 2016; Kayfetz and Kimmerer 2017). *Acartiella sinensis* is also a common food item for the endangered Delta Smelt as well as the more abundant American Shad (Appendix A), mostly in summer and fall (Slater and Baxter 2014; Slater et al. 2019).

Since the introduction of *A. sinensis* in 1993, the zooplankton assemblage in the low-salinity Suisun area has shifted in trophic composition. Once dominated by herbivorous cladocerans and copepods such as *E. affinis* and *P. forbesi*, the community has become more "top-heavy" with the spread of *A. sinensis* (Kratina et al. 2014; Kratina and Winder 2015). The sustained prevalence of *A. sinensis* in the low-salinity zone and its high predation rate on the nauplii of *P. forbesi* is linked to a shift in the spatial distribution of *P. forbesi* out of the low-salinity zone and upriver into more freshwater habitats (Kayfetz and Kimmerer 2017). This shift in *P. forbesi* distribution could have implications for the majority of planktivorous fishes that feed on the calanoid copepod populations.

Materials and Methods

Zooplankton data

The data used for these analyses were obtained from an integrated database of five long-term zooplankton monitoring surveys in the upper estuary. These include the Environmental Monitoring Program (EMP), 20-mm Survey (20mm), Fall Midwater Trawl (FMWT), Summer Townet (STN), and Fish Restoration Program monitoring (FRP). These surveys are described in detail in Kayfetz et al. (2020) and Bashevkin et al. (2022). Briefly, EMP samples monthly year-round since 1972, 20mm samples every other week March through July since 1995, STN samples every other week June – August since 2005, FWMT samples monthly September through December since 2011, and FRP samples annually to monthly near tidal marshes (or areas soon to be restored to tidal marshes) March through December since 2015. Each survey samples at a set of fixed stations (Fig. 2). EMP also samples at a set of moving stations at locations where the bottom conductivity is 2 and 6 mS/cm. Many of these surveys collect other parameters such as fish abundance or water quality, but only the time period of zooplankton sampling is described above. Furthermore, sampling locations and frequencies have changed over time (Kayfetz et al. 2020; Bashevkin et al. 2022).

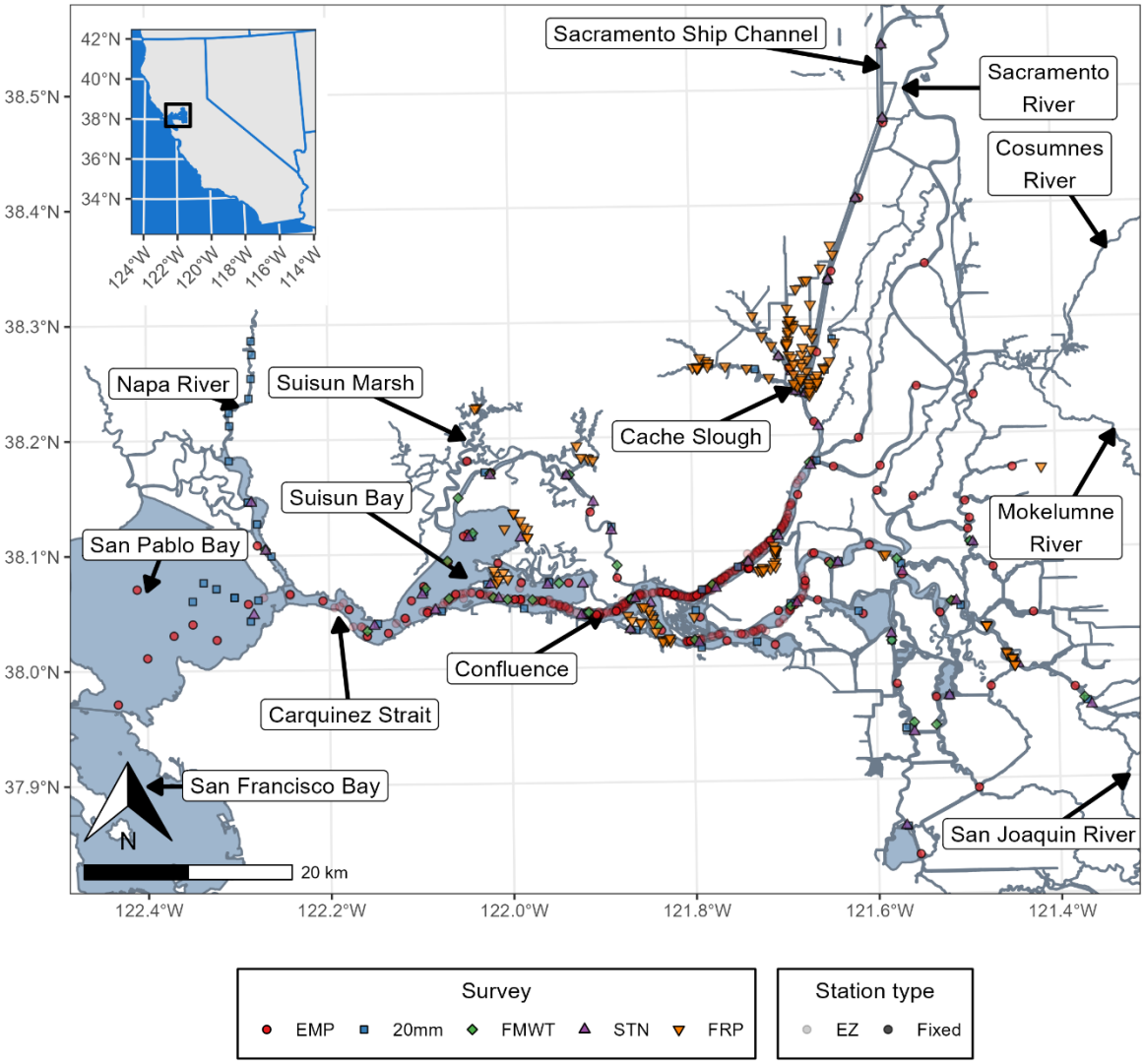

246

247 Figure 2. Map of the study area, depicting all sampling stations. Survey abbreviations are as follows: EMP =
248 Environmental Monitoring Program, 20mm = 20-mm Survey, FMWT = Fall Midwater Trawl, STN = Summer
249 Townet, FRP = Fish Restoration Program. The EMP survey has some non-fixed stations that move with the
250 salinity field and are depicted here with increased transparency.

251 The data from each survey are integrated by the R package zooper (Bashevkin 2021),
252 which imports and standardizes the data from each survey. For the purposes of these
253 analyses, we selected data from the mesozooplankton size-class, which corresponds to
254 samples from the modified Clarke-Bumpus nets used by each survey, with mesh sizes of 150
255 – 160 µm. We selected all available data from each of our study species without missing
256 values in our covariates. When possible, adults and juveniles were analyzed separately since

these distinct life stages have different behaviors and abundance drivers and play distinct demographic roles. *Acartiella sinensis* was introduced to the estuary in 1993 (Orsi and Ohtsuka 1999), but adults were first counted in samples in 1994 and juveniles were first counted in 2006. Thus, adult data were filtered to the start date of 1994 and juveniles to the start date of 2006. For the other species, only adult data were available at the taxonomic resolution of our analysis. The final dataset had 33,255 samples for *B. longirostris* adults, 32,026 samples for *Acanthocyclops* spp. adults, 17,189 samples for *A. sinensis* adults, and 11,224 samples for *A. sinensis* juveniles.

Exploratory data visualization revealed tighter relationships of each species' abundance with log-transformed salinity than raw salinity values. Thus, salinity was natural log-transformed for analyses. Furthermore, we standardized all covariates (including log-transformed salinity) by subtracting the mean and dividing by the standard deviation. Lastly, since many of the sampling stations from the different surveys were nearby one another (Fig. 2), we clustered all stations into groups within a 1 km radius.

Model structure

We fit Bayesian generalized additive mixed models with the R package brms (Bürkner 2017; Bürkner 2018), which uses the Bayesian modeling platform Stan (Stan Development Team 2021), as well as the R package mgcv (Wood 2011) to construct the generalized additive model smoothers. Smoothers enable the modeling of non-linear relationships of arbitrary shape; they make no assumptions about the shape of the curve. They can thus be used to model unimodal curves such as the relationship between salinity and abundance, multimodal curves such as interannual trends in abundance, and cyclical curves such as seasonal patterns. Smooths are constructed with different types or combinations of splines, which produce the modeled curves. Splines are smooth functions constructed from a number of component basis functions. The "wiggliness" of the spline is controlled by the

basis dimension (k), which controls the maximum number of basis functions in the spline. Thus, splines with higher basis dimensions are allowed to produce more wiggly curve shapes, while lower basis dimensions are constrained to smoother curve shapes. Similar to interactions among effects in linear models, splines can also interact with one another. In this case, spline interactions produce a multi-dimensional smoothed surface in which the interactions themselves are also nonlinear, rather than the 1-dimensional curves that would be produced without interactions.

Models were fit with a hurdle lognormal distribution, using the catch per unit effort (CPUE; organisms m^{-3}) of the specified taxon and life stage as the response variable. Hurdle models account for excessive 0s in the response by separately modeling the probability of absence (0 CPUE, referred to as the hurdle probability) and the probability of the non-zero values (i.e., abundance given presence).

We initially explored a wide range of model structures on the *B. longirostris* data to determine the structure that best fits the data and best addresses our questions. We evaluated models with polynomials instead of splines, year and salinity coded as categories or continuous metrics, different combinations of our predictors, the hurdle probability modeled with a simple intercept or an effect of salinity, and the covariance matrix of the station cluster random intercepts constrained to the within-water distance matrix between station cluster locations. Model fit was evaluated for each option (see below) and compared to one another with leave-one-out cross-validation using the R package loo (Vehtari et al. 2017). We did not evaluate models with different basis dimensions (wiggliness parameters) since those values were determined a priori based on the resolution at which we wanted to model the data (see justifications below) and our understanding of the data collection methods and species cycles (e.g., it would not have made since to attempt to model daily seasonality when most surveys collect data monthly). Furthermore, increasing the basis dimensions above the values we

307 chose would have resulted in computationally infeasible models since the number of
308 parameters would have been vastly increased. We selected the final model structure among
309 those with good fit metrics as the best combination of parsimony and leave-one-out cross-
310 validation information criteria (i.e., it had the best criteria or equivalent criteria to more
311 complex structures).

312 Our overall approach in the final model structure was to model the probability of
313 presence with a smoothed function of salinity, and the non-zero abundances with smooth
314 functions of day of year, salinity, year, and their interactions, while accounting for space with
315 a random intercept for each station. Our combination of a Bayesian method, which
316 propagates uncertainty and handles unbalanced data, with a generalized additive model
317 approach, which accounts for key covariates like salinity and seasonality, allowed us to
318 resolve inconsistencies in the sampling designs, and incorporate both fixed stations and
319 stations that move with the salinity field.

320 The hurdle probability (probability of 0 CPUE) was modeled with a cubic regression
321 spline of salinity with a low basis dimension (k) of 5 since the relationship was expected to
322 have a simple unimodal shape. The abundance of *Acartiella sinensis* was so strongly seasonal
323 that we modified the hurdle component to also include seasonality. Thus, for *A. sinensis* we
324 modeled the hurdle probability with a two-dimensional tensor product smooth (i.e., an
325 interaction) of salinity (cubic regression spline, k=5) and day of year (cyclic cubic regression
326 spline, k=4). The basis dimension for day of year was also set low because we similarly
327 expected a simple shape of the relationship with absence probability.

328 The non-zero CPUEs were modeled with a three-dimensional tensor product smooth
329 (i.e., an interaction) of day of year (cyclic cubic regression spline, k=13), salinity (cubic
330 regression spline, k=5), and year (cubic regression spline, k=5). The basis dimension for day

of year was set to 13 to match the monthly nature of these sampling programs (since the smooth is cyclical, a basis dimension of 13 has 12 independent functions). The basis dimension for salinity was set to the low value of 5 because the relationship with salinity was expected to be a simple unimodal shape, and a basis dimension of 5 would still allow much greater complexity than a simple unimodal shape. The basis dimension for year was set to the low value of 5 because we were interested in evaluating broad long-term patterns, rather than fine-scaled year-to-year abundance trends. Thus, the results of this model represent broad long-term trends, not predicted abundances on specific years. For juvenile *A. sinensis,* the basis dimension for year was reduced to 3 since they have only been counted in samples since 2006 and thus the time series is shorter. We also included a random intercept for each station cluster.

We fit separate models on each species and life stage (4 total). Models were run on three chains, each for 5,000 iterations including 1,250 used for the warmup that were then discarded. We used weakly informative priors as recommended by the Stan authors (Stan Development Team 2021). These priors aid model fitting by providing more probability to more reasonable parameter values but are weak enough to be overwhelmed by a reasonable amount of data. Some prior distributions use the familiar mean and standard deviation, but others do not have those values defined and instead use the location (the central tendency of the distribution) and scale (the spread of the distribution) parameters. Our priors were as follows for each parameter type:

Abundance intercepts: Normal distribution with location 0 and standard deviation 10

Hurdle intercepts: Logistic distribution with location 0 and scale 1

Slopes: Normal distribution with mean 0 and standard deviation 5

Random intercept standard deviations: Half-cauchy distribution with location 0 and scale 5.

Spline standard deviation: Student t distribution with 3 degrees of freedom, mean 0, and scale 4.7.

Each model was validated and checked prior to use. All models were inspected to ensure adequate sampling by verifying the posterior effective sample size (> 100 per chain) and Rhat values (< 1.05) (McElreath 2015). We further inspected visual plots comparing the model outputs to the raw data to ensure they matched. These plots included the proportion of zero values, the distribution of non-zero CPUE values, and the predicted non-zero CPUE values for each row in the dataset. We also inspected the spatiotemporal variograms for spatiotemporal autocorrelation using the R package gstat (Pebesma 2004; Gräler et al. 2016). We detected some residual autocorrelation, and thus used a conservative significance threshold of $p < 0.01$ to account for any potential impacts.

Model predictions

We visualized predicted values from the models to explore the abundance patterns of each species and life stage. Predicted values were generated over a range of covariates that included all combinations of 6 evenly spaced time-points per month (from 1972 to 2019) and a series of salinity values selected as quantiles from the raw data (every 0.05 from 0.05 to 0.95). Since there were some gaps in the time series (e.g., winters were not sampled some years in the 1970s and 1980s), those same gaps are preserved in the model predictions to avoid extrapolation. Model predictions were then plotted along with their 99% credible intervals. To visualize the multidimensional model outputs, we created three plots for each set of model predictions. Each plot had one of the covariates (salinity, day of year, or year) on the x-axis while the other two variables were illustrated with color or separate plots. For the

two covariates included as color or separate plots, we chose a subset of the previously selected quantiles used in generating model predictions in order to reduce plot complexity and aid interpretation. These values were chosen as an evenly spaced subset of the values available. For example, for plots with salinity on the color scale, we chose salinity quantiles of 0.05, 0.35, 0.65, and 0.95, (i.e., the 4 evenly spaced quantiles along the range we used).

To explore spatial patterns in abundance, we extracted the mean estimated value from each station cluster random intercept. These values were then plotted over a map of the study region.

Code availability

The code used in these analyses is available at https://github.com/sbashevkin/SDP.

Results

Bosmina longirostris adults

The abundance of adult *B. longirostris* has regularly peaked in the spring between April and May. In earlier years, another large peak occurred in the late summer to fall between August and October. In some years (1980 and 1985), this fall peak was as large as the spring peak. However, by 1990, the fall peak was greatly reduced to just a small increase, which has since continued to decrease in size, becoming non-existent by 2015 (Fig. 3).

Bosmina longirostris adults were most abundant in freshwater, and abundance decreased as salinity increased (Fig. S1). In the salinity of 1.113, the fall peak was larger than the spring peak in earlier years. However, the fall peak at this and lower salinities was greatly reduced by 1995, shrinking smaller than the spring peak even as the overall abundance in this salinity continued to decrease over time (Fig. 3, S1).

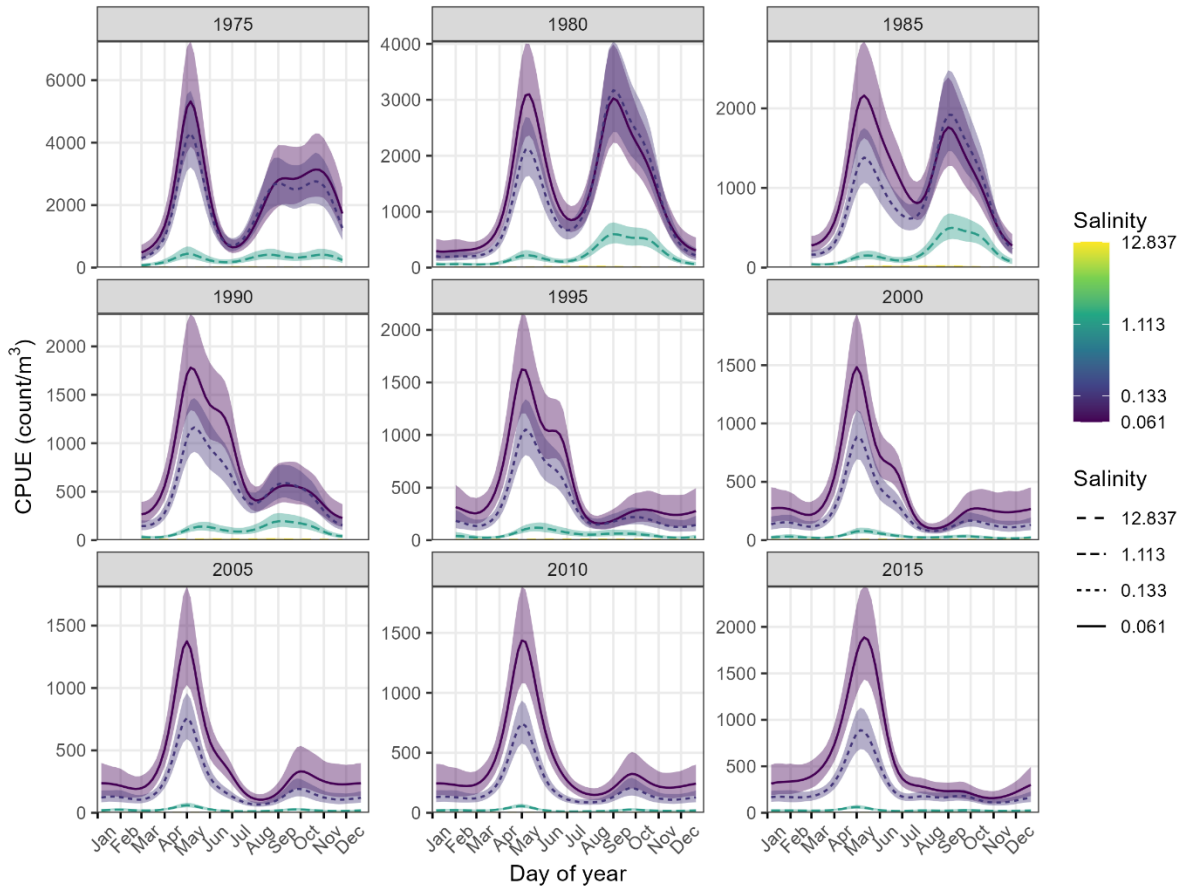

Figure 3. Seasonal patterns in *Bosmina longirostris* adult abundance with 99% credible intervals. Each plot represents predictions from different position on the smoothed yearly trend, which was restricted in its "wiggliness" to favor capturing the long-term trends over year-to-year swings in abundance. Thus, the plots for each year may not represent exact conditions for that year, but rather the average abundance for a few years before through a few years after the year portrayed. Predictions for different salinity values are represented by line and shading color, which is on the log scale, as well as line type. The y-axis limits differ among plots to facilitate comparison of seasonal trends. Absolute trends in abundance over time are represented in Fig. 4. Missing values (e.g., the months of Jan, Feb, and Dec in 1975) represent gaps in the raw data. Salinity is reported on the Practical Salinity Scale.

The abundance of adult *B. longirostris* has declined in most months. This is most apparent in August through November, corresponding to the loss of their former fall peak. In some months, their abundance has mostly decreased over time except in recent years which have a slight uptick. This recent uptick appears in January through March and May through July but is most significant in May through July (Fig. 4).

Controlling for all other factors (salinity, year, month), *B. longirostris* adult abundance was highest in the Southeastern Delta. Other areas around the boundaries of the sampled area also had higher abundances such as San Pablo Bay, Napa River, and parts of the Cache Slough Complex and Sacramento Deep Water Ship Channel. The Sacramento River corridor between Cache Slough and Suisun Bay generally had low abundance, as did parts of the Northeastern Delta (Fig. 5).

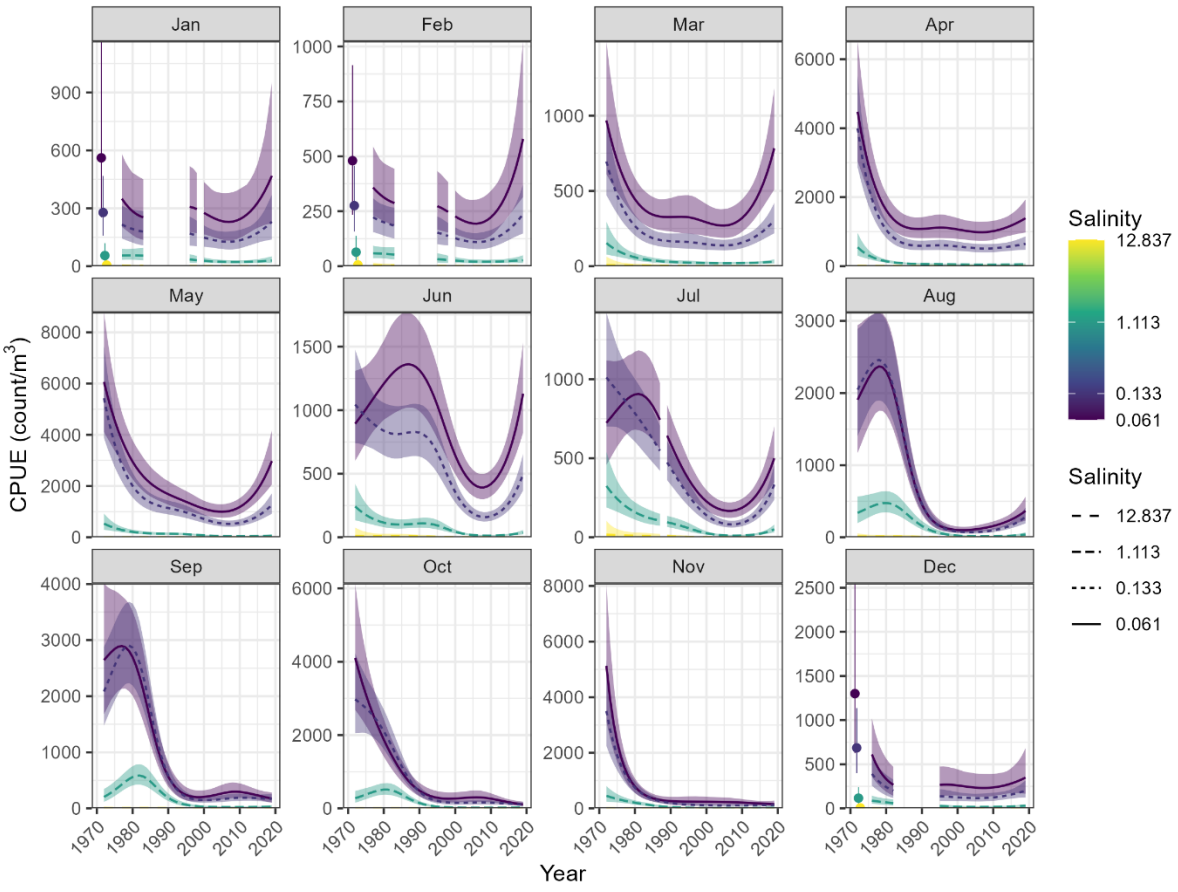

Figure 4. Yearly patterns in *Bosmina longirostris* adult abundance with 99% credible intervals. Each plot represents the pattern for a separate month. Predictions for different salinity values are represented by line and shading color, which is on the log scale, as well as line type. The y-axis limits differ among plots to facilitate comparison of long-term trends. Seasonal trends in abundance are represented in Fig. 3. Missing values represent gaps in the raw data. Salinity is reported on the Practical Salinity Scale.

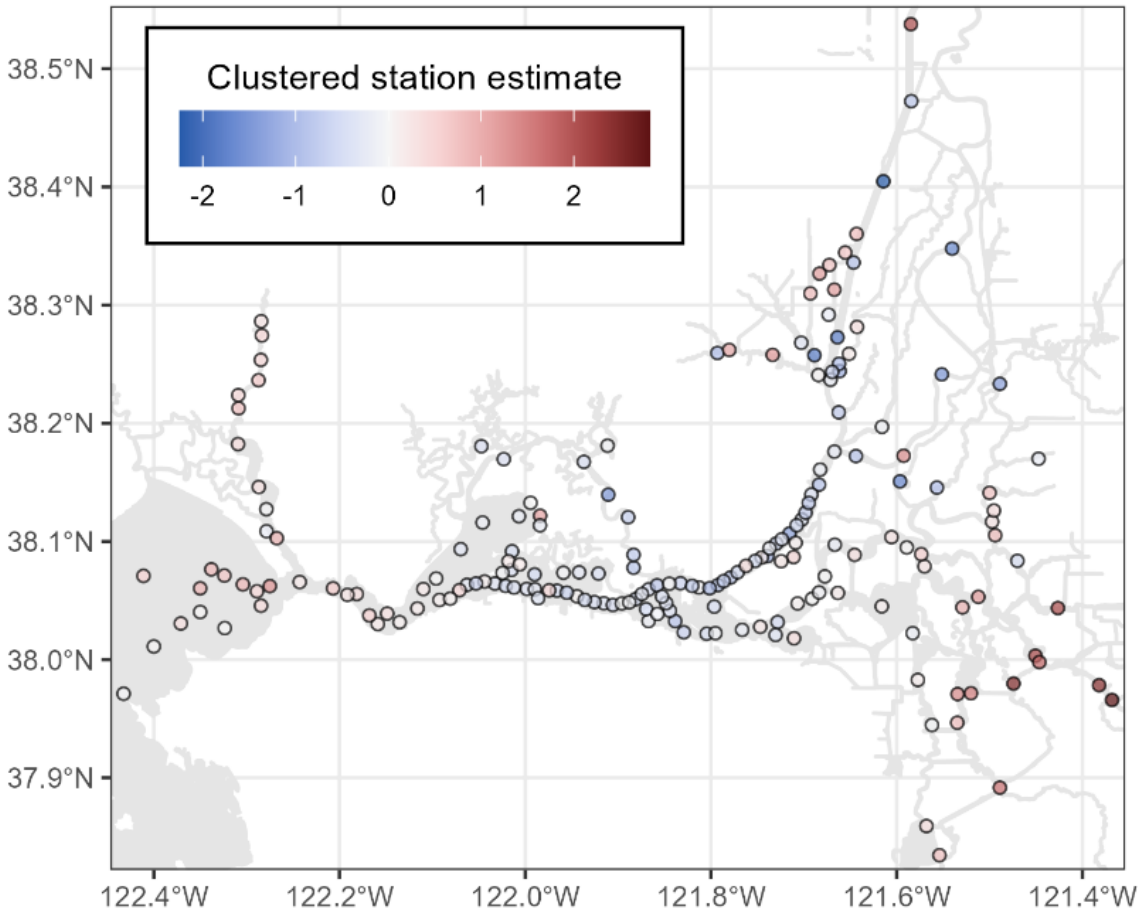

Figure 5. Estimated values of the random intercepts for station clusters in the *Bosmina longirostris* adult model. Stations within 1 km were clustered into groups, plotted here as separate points. Point color indicates whether each station cluster has higher or lower *B. longirostris* adult abundance, after controlling for the other covariates (day of year, salinity, and year).

Acanthocyclops spp. adults

The abundance of *Acanthocyclops* spp. adults has peaked regularly in the spring from April to May in all years. This peak was apparent in the two lower salinity levels (0.062 and 0.137) but generally not in the two higher salinities (1.402 and 13.017). In the second highest salinity of 1.402, abundance peaked in the winter from February through March in most years, although limited sampling in these months in some years may have masked the signal (Fig. 6).

In the earlier years (before ~2000), *Acanthocyclops* spp. were most abundant in the lower salinities, peaking around 0.3. Abundance decreased on either side of that peak but fell much lower in the highest salinities (Fig. S2). Over time, the relationship of *Acanthocyclops* spp. with salinity leveled out such that they became equally abundant in all salinity levels in most months (Fig. S2).

The abundance of *Acanthocyclops* spp. has dramatically declined over time in all months. There was a slight uptick in the 1980s to 1990s in most months, but populations crashed again after this period (Fig. 7). Overall trends in January and February were mostly flat with generally low abundance in all years but the missing data in those months may be obscuring patterns.

The highest *Acanthocyclops* spp. abundance after controlling for the other covariates was in Cache Slough, Suisun Marsh, the Southeastern Delta, Carquinez Strait, San Pablo Bay, and the Napa River. The lower Sacramento and San Joaquin rivers through Suisun Bay generally had lower abundances, as did most of the western-most areas (Fig. 8).

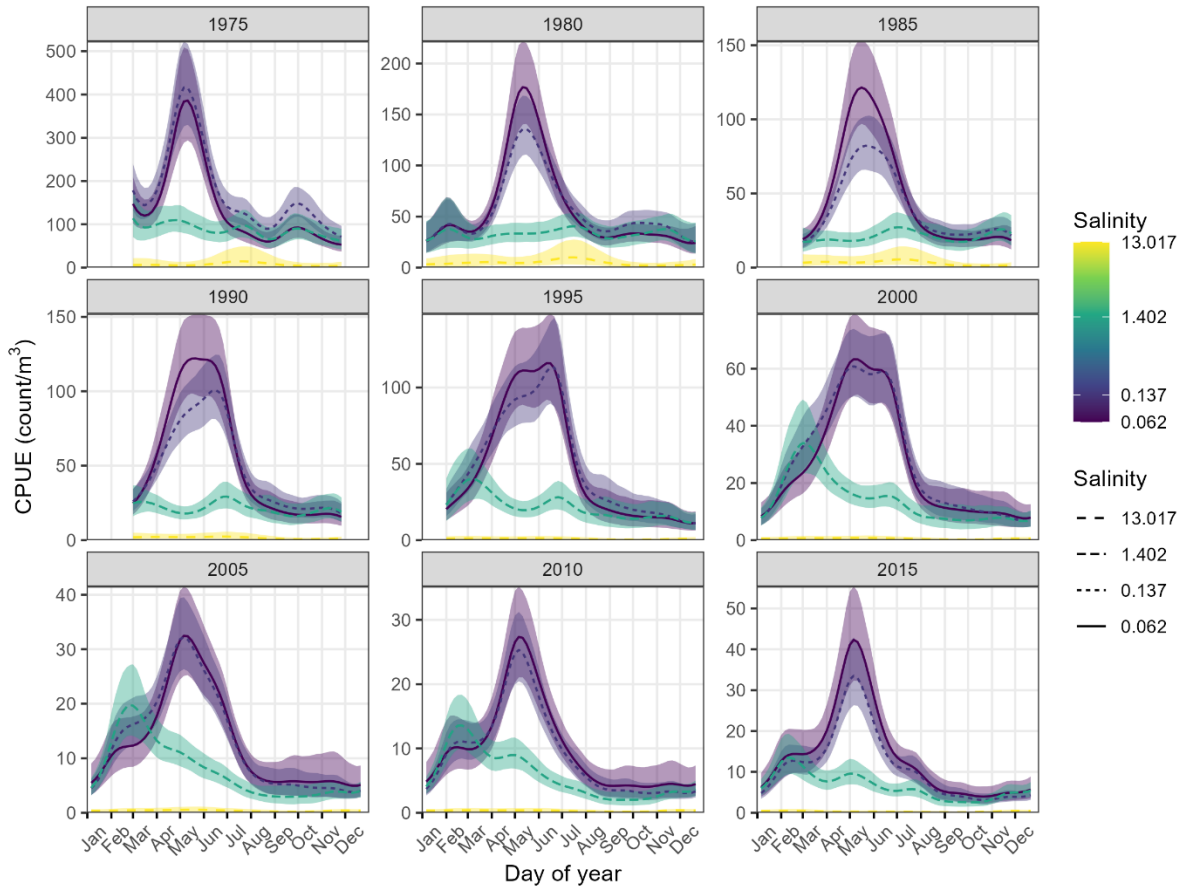

453

454 Figure 6. Seasonal patterns in *Acanthocyclops* spp. adult abundance with 99% credible intervals. See Fig. 3 for a

455 full description.

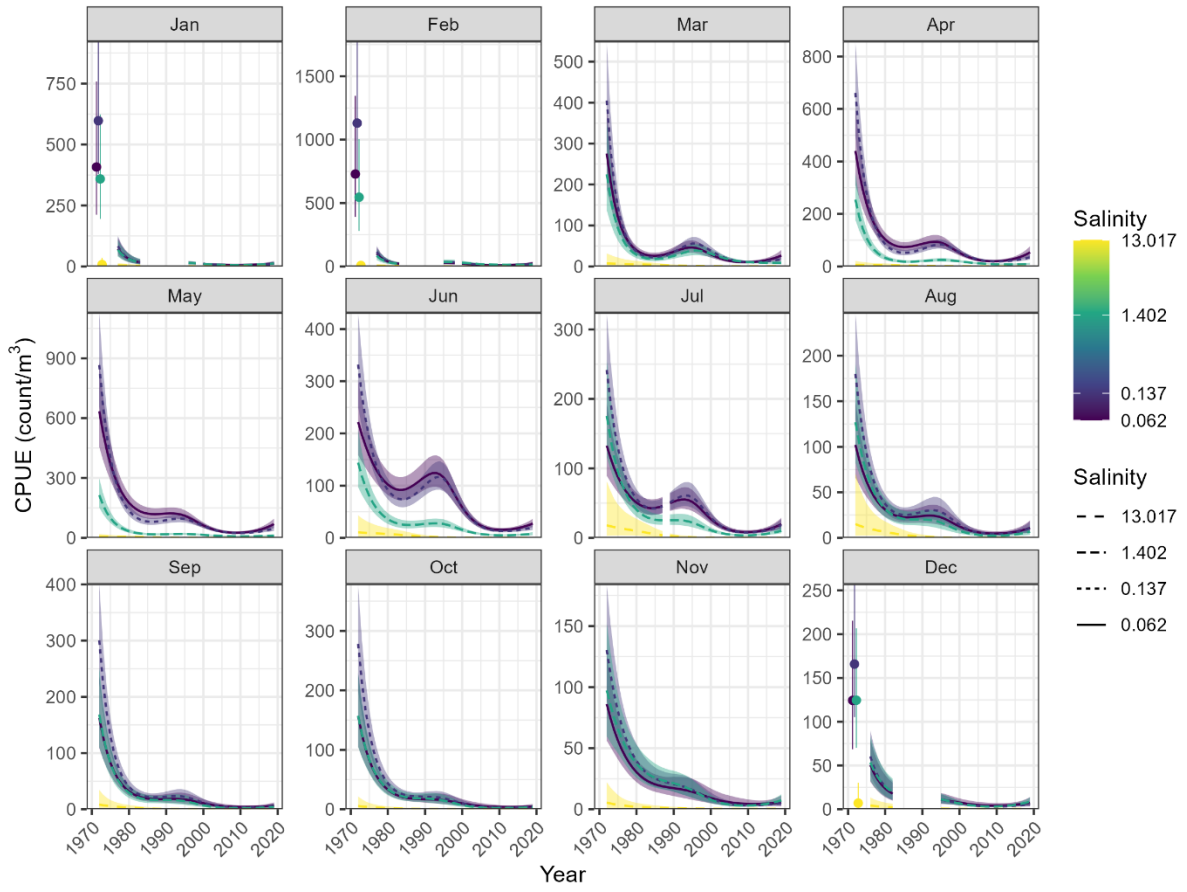

456

457 Figure 7. Yearly patterns in *Acanthocyclops* spp. adult abundance with 99% credible intervals. See Fig. 4 for a

458 full description.

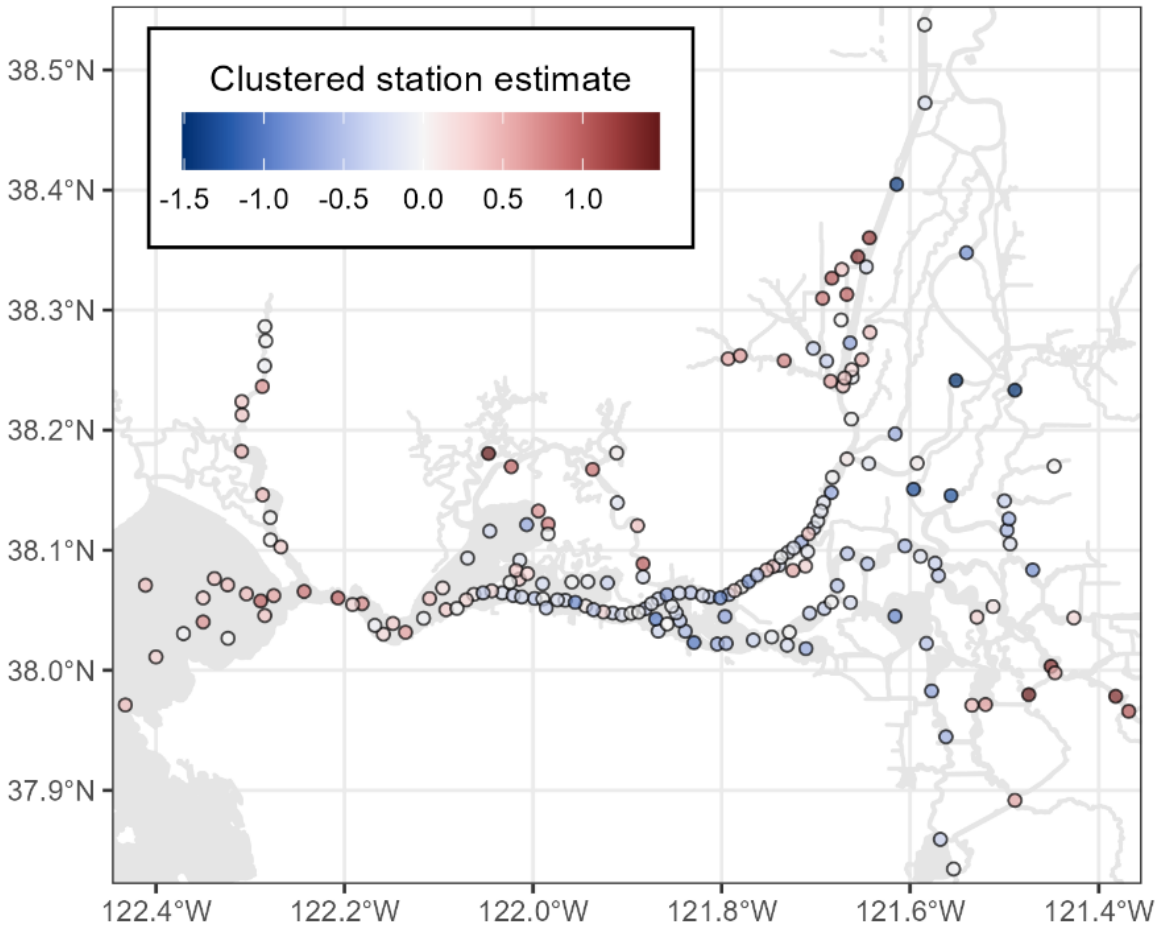

Figure 8. Estimated values of the clustered station random intercepts for *Acanthocyclops* spp. adults. See Fig. 5 for a full description.

Acartiella sinensis adults

Acartiella sinensis had the strongest seasonality of the three species investigated. Adults peaked in the fall from August through December with the highest levels in September and October. Abundances then dipped close to zero from February through May (Fig. 9).

Adult *A. sinensis* were most abundant in salinities between about 1 and 4. The effect of salinity on abundance has increased over time, especially in May through July where the peak was greatly reduced in earlier years (Fig. S3).

Unlike the other two species, *A. sinensis* adults did not exhibit any overall long-term decreases in abundance. However, the time series was shorter, only starting in 1994. In most months, the most recent abundance was similar to the earliest abundance level, but abundance did increase over time in March through July. The abundance peaked in the 2010s in most months and some months also had an earlier peak around 2000 (Fig. 10).

Spatially, *A. sinensis* adult abundance was highest (controlling for all other covariates) along the corridor from the lower Sacramento River just below Cache Slough all the way through to Carquinez Strait. The Southeastern and Northern Delta had the lowest abundances (Fig. 11).

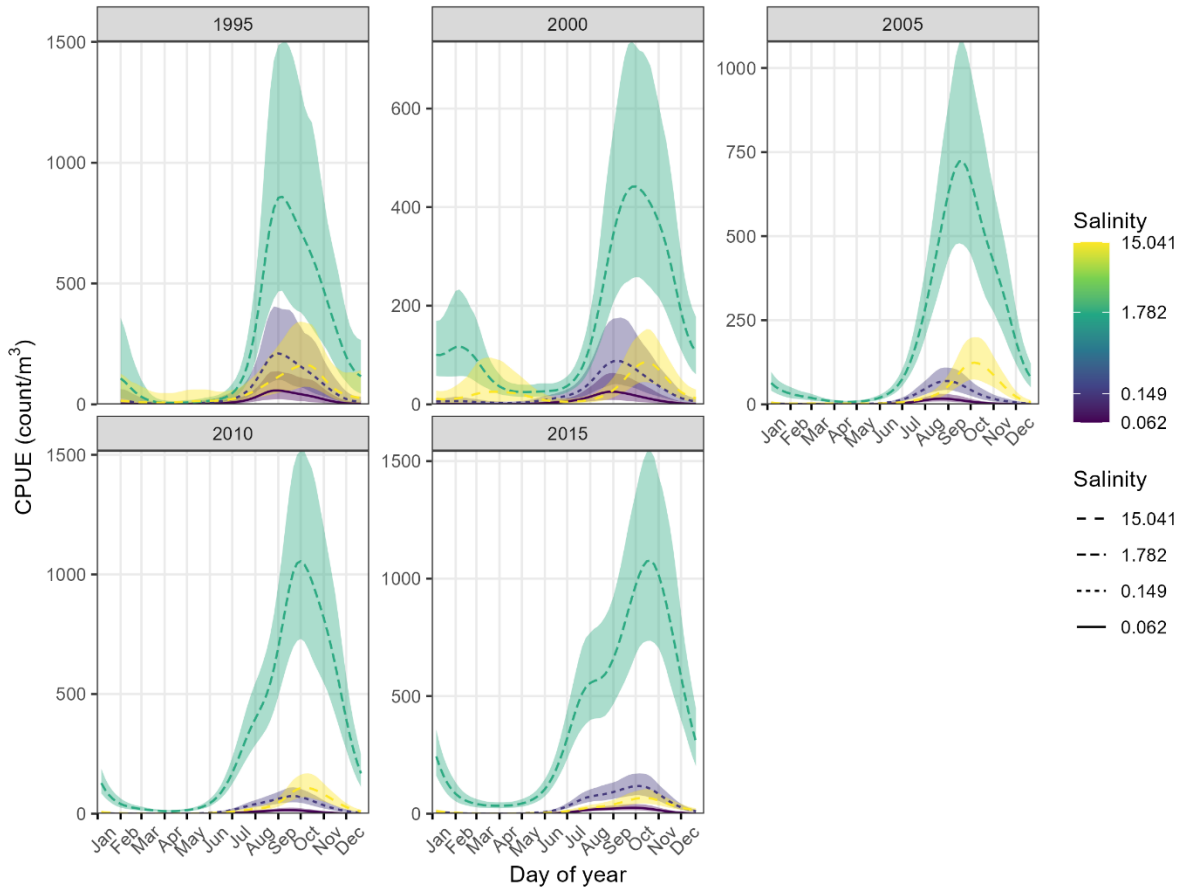

Figure 9. Seasonal patterns in *Acartiella sinensis* adult abundance with 99% credible intervals. See Fig. 3 for a full description.

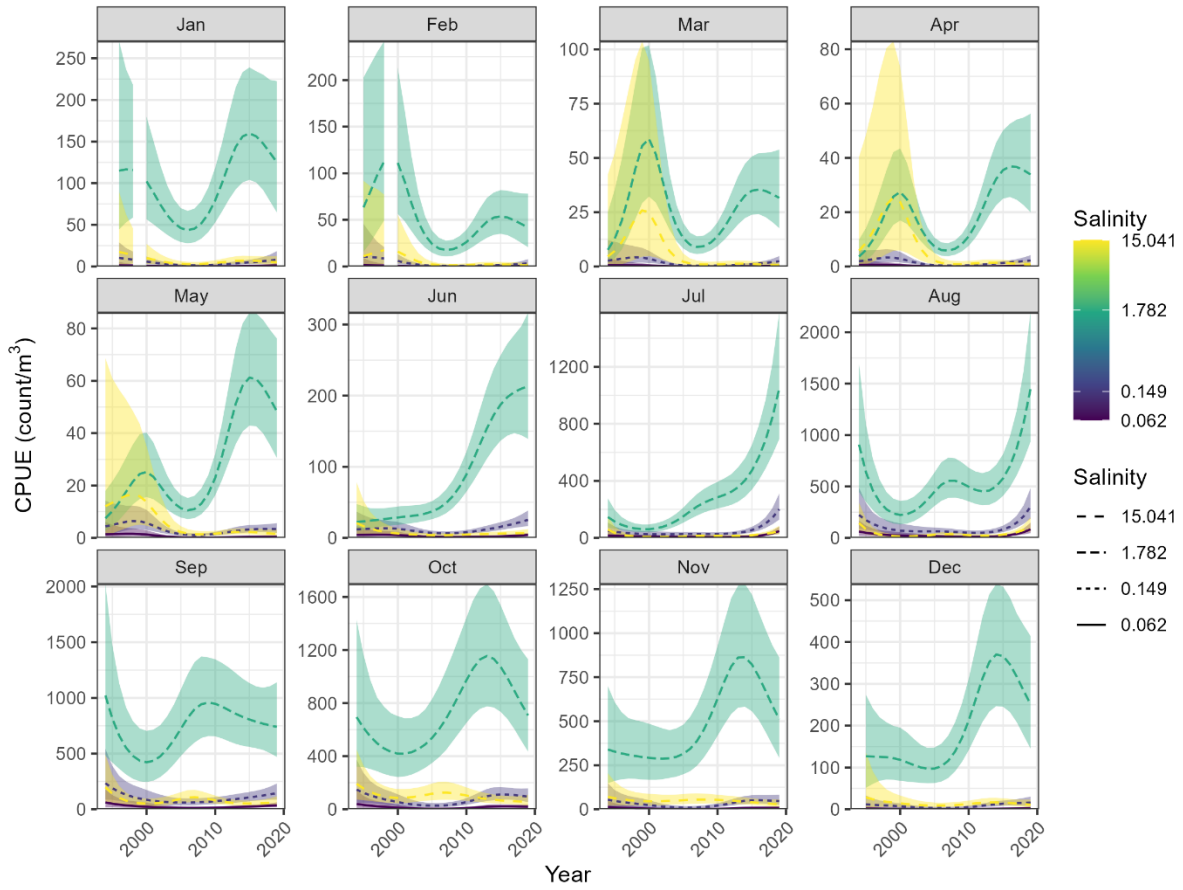

Figure 10. Yearly patterns in *Acartiella sinensis* adult abundance with 99% credible intervals. See Fig. 4 for a full description.

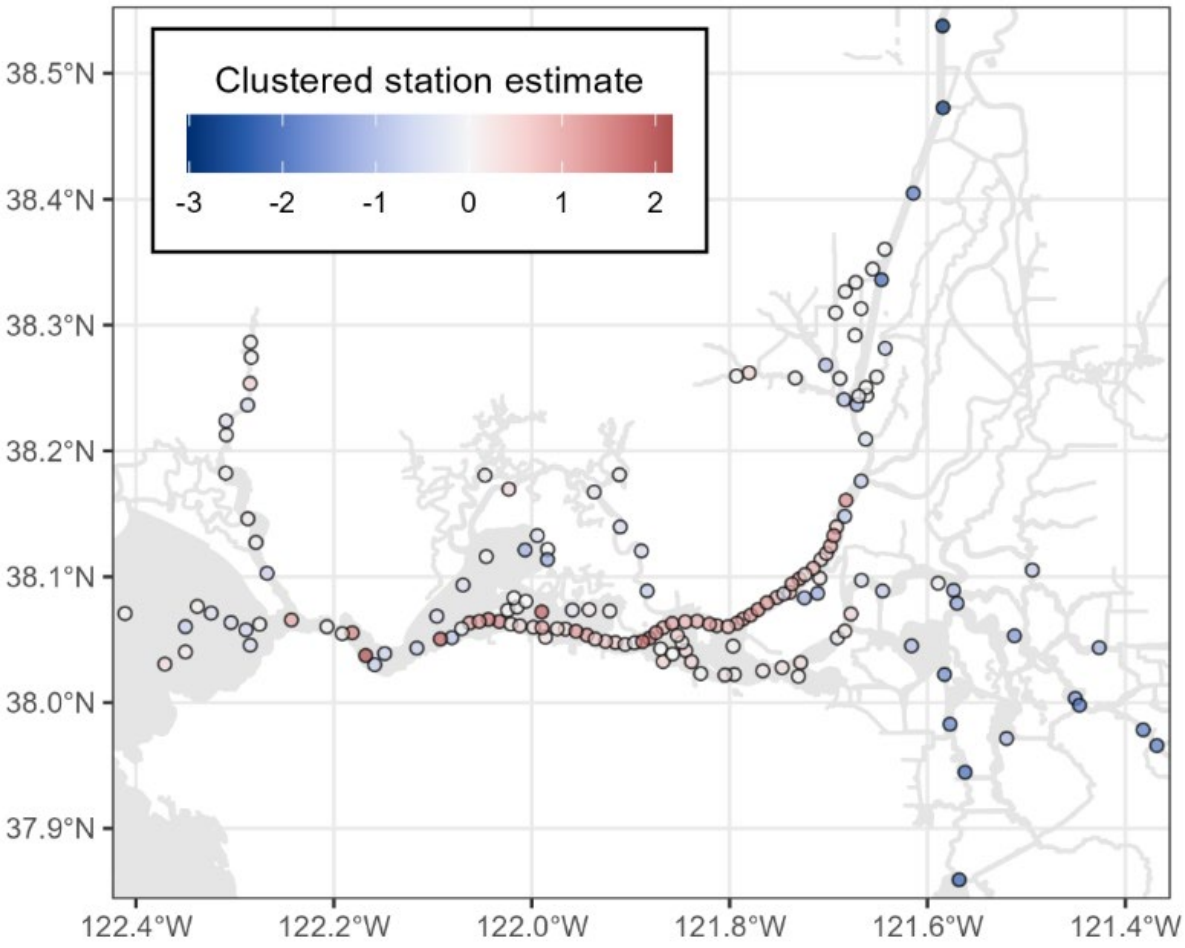

Figure 11. Estimated values of the clustered station random intercepts for *Acartiella sinensis* adults. See Fig. 5 for a full description.

Acartiella sinensis juveniles

Like the adults, juvenile *A. sinensis* also had strong seasonal abundance patterns, peaking over just a few months and then subsiding to close to zero abundance. Peaks occurred in the summer from July through September, but the width of the seasonal peak grew over time. Around 2006 they were abundant for just 2 months (July and August) while from about 2015 to 2018 they were abundant from April through November (Fig. 12).

Acartiella sinensis juveniles were abundant in higher salinities > 4 but declined at the very highest salinities close to 16. Their abundance in lower salinities increased over time but always remained lower than their abundance at the higher salinities (Fig. S4). In most years,

497 the seasonal abundance peak was 1-2 months later at the highest salinity of ~16 than the other
498 salinity levels (Fig. 12).

499 While the time series was much shorter (2006 – 2020) for *A. sinensis* juveniles than
500 any of the other species and life stages investigated, we did detect some long-term trends in
501 some months. The trends were most apparent in the second highest salinity of 2.703 where
502 they were most abundant. Abundance increased over time in April through June and
503 decreased over time in August. This corresponds to the widening of the seasonal peak over
504 time. The other months generally did not have any significant long-term trends (Fig. 13).

505 The spatial pattern of *A. sinensis* juveniles was less clear than the other species and
506 life stages. However, they were generally most abundant along the San Joaquin River
507 corridor in the Southern Delta and in some Suisun Bay stations. They were least abundant in
508 the lower Sacramento River between Cache Slough and the Confluence, as well as in the
509 Napa River and Eastern Suisun Marsh (Fig. 14).

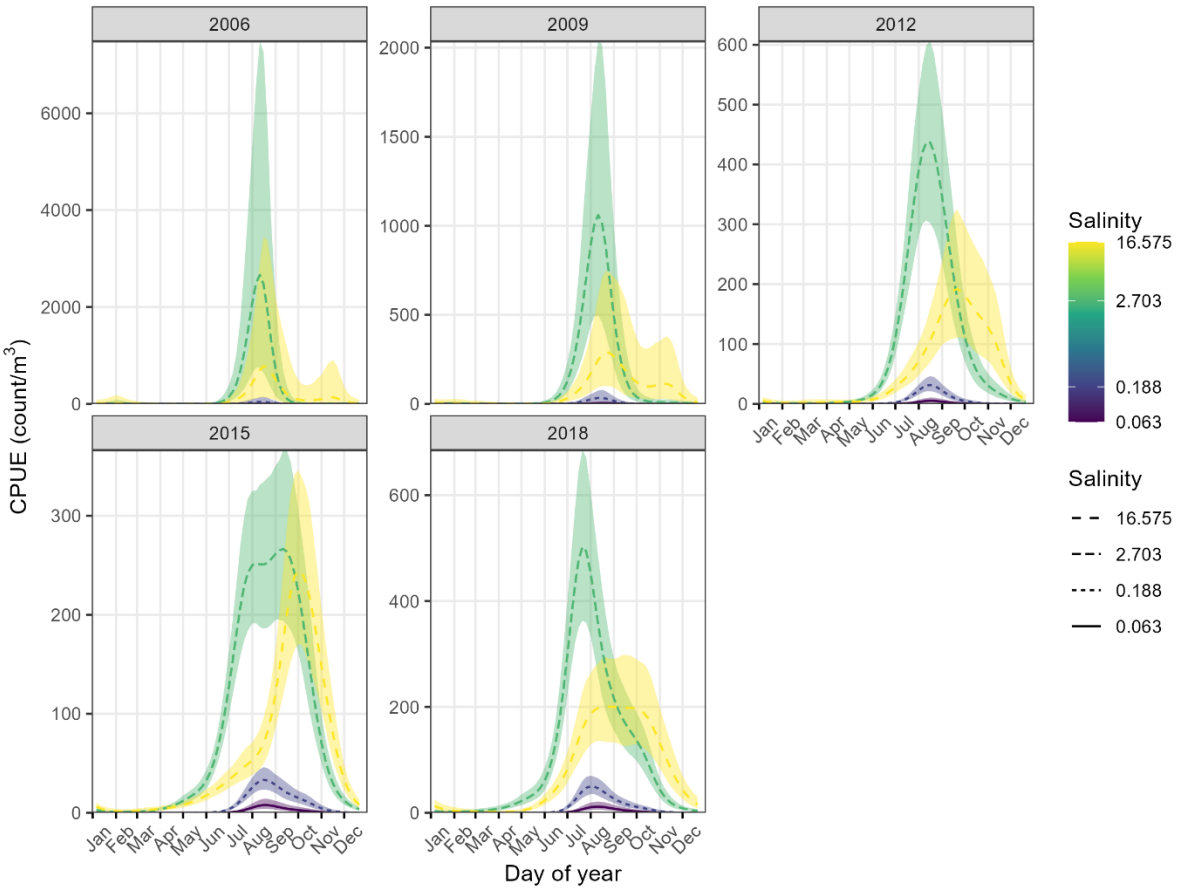

510

511 Figure 12. Seasonal patterns in *Acartiella sinensis* juvenile abundance with 99% credible intervals. See Fig. 3

512 for a full description.

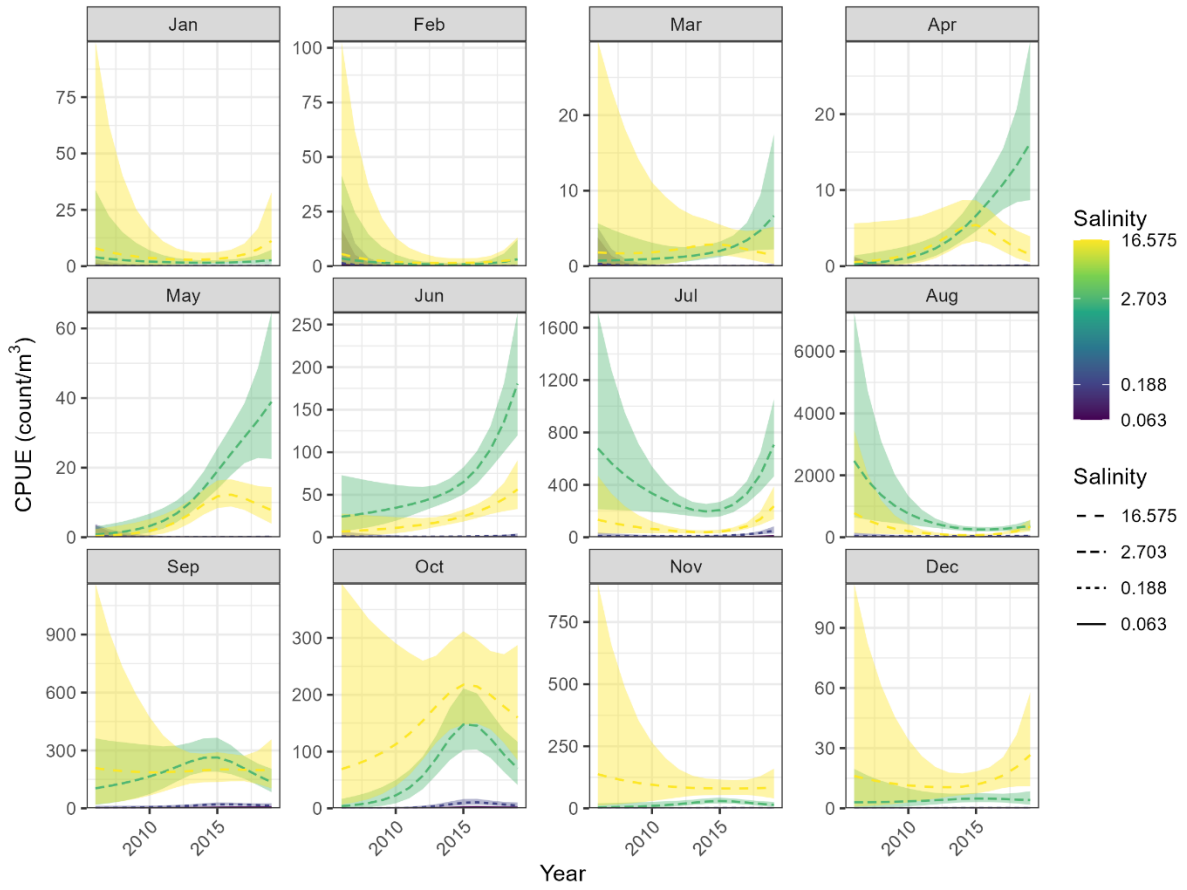

513

514 Figure 13. Yearly patterns in *Acartiella sinensis* juvenile abundance with 99% credible intervals. See Fig. 4 for a

515 full description.

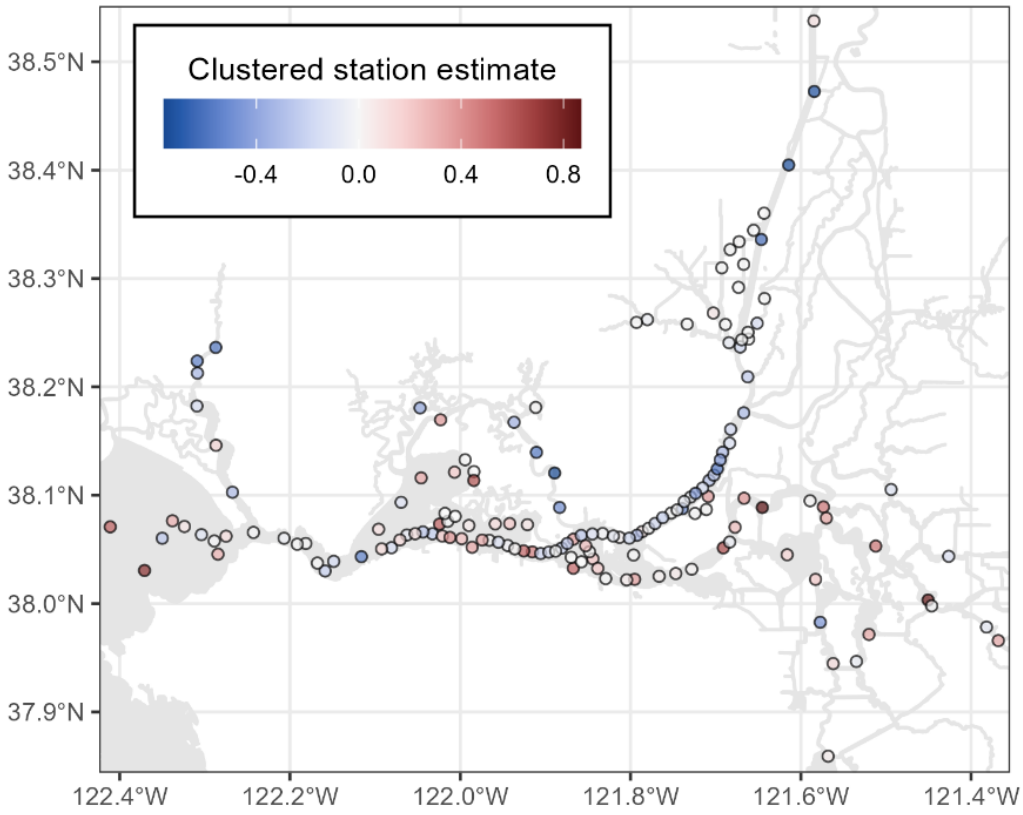

516

517 Figure 14. Estimated values of the clustered station random intercepts for *Acartiella sinensis* juveniles. See Fig.
518 5 for a full description.

519 ## Discussion

520 We found marked changes in the seasonality and overall abundance of three key
521 zooplankton taxa in the upper estuary. *Bosmina longirostris* no longer peaks in abundance in
522 the fall months, *Acanthocyclops* spp. dramatically declined in all months and lost its strong
523 relationship with salinity, and *A. sinensis* adult abundance has become more strongly related
524 to salinity while juveniles have developed wider abundance peaks. In this process, we have
525 documented the relationship of each species with salinity and seasonality back to the
526 beginning of monitoring or their introduction, increasing our understanding of their ecology
527 and importance in the estuary.

Seasonal abundance patterns

Currently, *B. longirostris* and *Acanthocyclops* spp. adults peak in the spring while *A. sinensis* adults peak in the fall and juveniles peak in the summer. The spring peaks line up with the spawning of Delta Smelt while the summer and fall peaks provide critical food for Delta Smelt juveniles and young-of-the-year (Slater and Baxter 2014; Slater et al. 2019). The spring peaks also correspond to the outmigration of juvenile salmon and could provide important food necessary to increase growth rates (Herbold et al. 2018; Phillis et al. 2018; Zeug et al. 2019) and reduce oceanic predation risks since larger fish have lower predation risk (Sogard 1997).

Salinity abundance patterns

Bosmina longirostris and *Acanthocyclops* spp. are also both most abundant in the lowest salinity bins (salinity < ~ 1), although *Acanthocyclops* spp. has a broader and higher salinity range potentially due to the different tolerances of the species in the complex. Freshwater habitat, especially in the spring, is where spawning for most native fish species occurs, including Delta Smelt and Sacramento Splittail (Moyle 2002). *Acartiella sinensis* peaks in more saline water (~1-4) corresponding to the low salinity zone, which is a key habitat for rearing Delta Smelt (Sommer and Mejia 2013). Juvenile *A. sinensis* have a narrower salinity range and are abundant in more saline waters than the adults. The brackish and low salinity habitats are important rearing habitats for many native fishes that evolved in highly variable conditions, giving native fishes an advantage over non-native fishes (Moyle et al. 2010), so an abundance of *Acanthocylops* spp. in brackish habitats may provide important food for rearing native fish. Both *Acanthocyclops* spp. and *A. sinensis* are found in the diets of Longfin Smelt (Appendix A), which spawn and rear at slightly higher salinities than many other native fishes (Hobbs et al. 2006; Grimaldo et al. 2017; Jungbluth et al. 2021).

552 Interestingly, abundance peaks of juvenile *A. sinensis* were regularly 1-2 months later
553 in the highest salinity (16.575) than in any of the lower salinities, which all peaked around the
554 same time. This may reflect movement of *A. sinensis* (either juveniles or reproductive adults)
555 into more saline waters from the late summer to fall. *Acartiella sinensis* exhibit tidal vertical
556 migration behaviors (Kimmerer et al. 2002) that, depending on their interactions with tidal
557 currents, could result in geographic movement or maintenance of a fixed geographic position.
558 Geographic movement seaward could result in the observed pattern, as could maintenance of
559 a fixed geographic position as salt intrudes further landward during the late summer to fall
560 (Enright and Culberson 2009).

561 ## Geographic abundance patterns

562 *Bosmina longirostris* and *Acanthocyclops* spp. had similar geographic patterns, with
563 their highest abundances (controlling for other covariates) in the Cache Slough Complex and
564 the southeastern and eastern boundaries of the study region. *Bosmina longirostris* especially
565 seemed to peak in areas of high residence time such as the northernmost location on the
566 Sacramento Ship Channel and areas in the East Delta (Vroom et al. 2017; Lenoch et al.
567 2021). The Sacramento Ship channel is an important last refuge for Delta Smelt and other
568 fishes (Young et al. 2021). *Acanthocyclops* spp. had very high geographic peaks in Suisun
569 Marsh and Cache Slough, both areas with remnant and restored tidal wetlands that are
570 important habitats for native fishes (Kimmerer et al. 2018; Colombano et al. 2020). They
571 both also had generally low abundance from Suisun Bay upstream (eastward) through the
572 lower Sacramento and San Joaquin Rivers, which was the region of highest abundance for *A.*
573 *sinensis* adults.

574 ## Long term changes

575 While *B. longirostris* and *Acanthocyclops* spp. have experienced overall declines in
576 abundance over time, *A. sinensis* has mostly increased, although over a shorter time period.

The declines of *B. longirostris* and *Acanthocyclops* spp. correspond to noted regime shifts and overall plankton declines across many species (Winder and Jassby 2011). *Acartiella sinensis* was introduced at the end of this regime shift and was not subjected to the same declines. The increase of *A. sinensis* could be related to expansion following its introduction as it fills niches (e.g., fall-abundant copepod predator in the low salinity zone) left by declining species.

The change to the seasonal pattern of *B. longirostris* may have been due to major environmental changes, including water operations and introduced species, but the precise mechanism is unclear. Prior to 1990, *B. longirostris* experienced two peaks, one in the spring and a second peak in the fall. In the late 1980s, *B. longirostris* abundance crashed during the fall. One potential explanation is changes to the operation of the State Water Project and Central Valley project. Project operations can significantly change flows in the San Joaquin River and the channels of the South Delta, where *Bosmina* is most abundant (Jassby et al. 2002; Jassby 2005). Exports from these water projects cause a decrease in residence time in the South Delta, particularly during the fall peak of *B. longirostris* (Hammock et al. 2019). Decreased residence time limits phytoplankton production, as well as directly exporting phytoplankton and zooplankton (Jassby et al. 2002; Hammock et al. 2019). However, decreases in residence time first became apparent during increases to exports in the late 1970s, which steadily increased from 1960-1980 before leveling off (Hammock et al. 2019), well before the disappearance of the fall peak of *B. longirostris*. While exports are highest in the fall, there was no major change to exports around the time of the loss of the fall *B. longirostris* peak, so the export explanation is unlikely to be the main factor driving the decrease.

Introduced species may be a more likely explanation for the change in the seasonal peaks of *B. longirostris*. The calanoid copepod *P. forbesi* was introduced in 1987 and quickly

602 became the most abundant calanoid in the system (Orsi and Walter 1991). *Pseudodiaptomus*
603 *forbesi* peaks in abundance from July through August, overlapping with the beginning of the
604 historical peak in *B. longirostris* abundance, and they occur in high abundances in low
605 salinities (Kayfetz and Kimmerer 2017), overlapping in salinity with *B. longirostris*.
606 *Pseudodiaptomus forbesi* may be competing with *B. longirostris* for food resources during
607 the fall during earlier years when most other zooplankton had peaked earlier in the year.
608 *Bosmina longirostris* and *P. forbesi* both eat a wide range of phytoplankton, bacteria, and
609 vascular plant detritus (DeMott and Kerfoot 1982; Acharya et al. 2005; Holmes and
610 Kimmerer 2022) and while direct competition is difficult to directly observe, it is a possible
611 explanation for the patterns we detected.

612 The dramatic decline of *Acanthocyclops* spp. abundance may be related to the
613 introduction of the cyclopoid *L. tetraspina* in 1993 (Orsi and Ohtsuka 1999). Before this
614 introduction, *Acanthocyclops* spp. was the most abundant cyclopoid in the region (Orsi and
615 Mecum 1986). After 1994, *L. tetraspina* quickly dominated the copepod community
616 (Hennessy 2018) with *Acanthocyclops* spp. averaging ~1% of the abundance of *L. tetraspina*
617 (Bashevkin et al. 2020). The introduction of *L. tetraspina* could have facilitated the decline of
618 *Acanthocyclops* spp. through facilitation of a common predator, *A. sinensis*, as it likely did
619 for *P. forbesi* (Kayfetz and Kimmerer 2017).

620 The relationship between *Acanthocyclops* spp. and salinity decreased over time.
621 Before 2000, they were most abundant at salinities around 0.3, and after 2000 they were
622 roughly equally abundant at a broad range of salinities from 0.6 to 3.4. This is likely due to
623 the differing salinity tolerances of the species within the complex and changes in the relative
624 abundances of those species over time. Unfortunately, we do not have data on the abundances
625 of each species in the complex so we cannot untangle the individual patterns. While *A.*
626 *vernalis* has been described as native to the estuary (Orsi and Mecum 1986; Kratina and

627 Winder 2015) in past literature, more recently the presence of the *A. vernalis* species complex
628 has been confirmed in the estuary (Jungbluth et al 2021). Thus, it is unknown which species
629 could be native, or if some were introduced during the study period. The strong relationship
630 with salinity in early years (Fig. S2) may be indicative of one or more species with lower
631 salinity tolerances initially dominating. Then, the diminishment of that relationship with
632 salinity in later years may have been caused by the introduction and expansion of higher
633 salinity species within the complex, such as *A. americanus* which has been found in high
634 salinity areas including the Mediterranean Sea (Alekseev 2021). The shift in phytoplankton
635 communities caused by the introduction of *Potamocorbula amurensis* (Lucas et al. 2016),
636 could also have contributed to this change by becoming the prime limiting abundance factor,
637 rather than salinity. A reduction in food quantity or quality could have reduced the salinity
638 abundance peak around 0.3, resulting in the flattening of the salinity-abundance relationship
639 that we observed after 2000.

640 Abundances of adult *A. sinensis* were more strongly related to salinity over time. In
641 the earlier years (before 2005), they were present in all salinities in our study and even
642 equally abundant in high salinities of 15 and low salinities of 0.15. They also exhibited a
643 unique winter-spring abundance peak in the two highest salinities that disappeared by 2005.
644 They were first detected in the estuary in 1993 (Orsi and Ohtsuka 1999), thus this pattern
645 could reflect them settling into their ecological niche over time.

646 Interestingly, *A. sinensis* juveniles had increasingly wide seasonal abundance peaks
647 over time, driven in part by differing timing of abundance peaks in the two highest salinity
648 bins. As noted above (Salinity abundance patterns), abundance peaks were regularly 1-2
649 months later in the highest salinity (16.575) than in the lower salinities. The abundance peak
650 of the highest salinity also grew relatively larger compared to the lower salinities over time,
651 which led to an overall widening of the seasonal abundance peak for *A. sinensis* juveniles.

However, the width of the abundance peak in each lower salinity level also seemed to increase over time. This demonstrates shifting phenology of *A. sinensis,* which could be caused by changes in the timing and location of reproduction, predation, or feeding. The zooplankton community has undergone many shifts over the history of this dataset (Orsi and Ohtsuka 1999; Winder and Jassby 2011), with *A. sinensis* potentially having its own impacts on lower trophic level zooplankton (Kayfetz and Kimmerer 2017). Since *A. sinensis* is predatory it could be following the abundance shifts of other species, resulting in changes to the location and timing of its reproduction, thus impacting the abundance of both adult and juvenile *A. sinensis*.

Conclusions

Many of the fishes in the estuary rely on zooplankton for at least part of their life cycle (Appendix A). Changes in prey resources can affect higher trophic levels by reducing the amount of available food or shifting the timing of peak abundance, thereby creating a mismatch between critical fish life stages and their prey. We found long-term shifts in all three of our study taxa. These shifts included changes in seasonality, relationships to salinity, and long-term abundance. Further studies investigating these patterns in additional species would be important to understand the past dynamics of zooplankton in the estuary. These results increase our understanding of the zooplankton community, which could inform the development of food web models and be matched to trends in fish abundance to examine the direct influence of declining zooplankton species on managed species.

References

Acharya K, Jack JD, Bukaveckas PA. 2005. Dietary effects on life history traits of riverine Bosmina. Freshwater Biology. 50(6):965–975. doi:10.1111/j.1365-2427.2005.01379.x.

Adamczuk M. 2016. Past, present, and future roles of small cladoceran *Bosmina longirostris* (O. F. Müller, 1785) in aquatic ecosystems. Hydrobiologia. 767(1):1–11. doi:10.1007/s10750-015-2495-7.

678 Adamczuk M, Mieczan T. 2019. Within-species phenotypic diversity enhances resistance to
679 stress - A case study using the polymorphic species *Bosmina longirostris*. International
680 Review of Hydrobiology. 104(5–6):137–146. doi:10.1002/iroh.201901985.

681 Alekseev V, Fefilova E, Dumont H. 2002. Some noteworthy free-living copepods from
682 surface freshwater in Belgium. Belgian Journal of Zoology. 132(2):133–139.

683 Alekseev VR. 2021. Confusing Invader: *Acanthocyclops americanus* (Copepoda:
684 Cyclopoida) and Its Biological, Anthropogenic and Climate-Dependent Mechanisms of Rapid
685 Distribution in Eurasia. Water. 13(10):1423. doi:10.3390/w13101423.

686 Ambler JW, Cloern JE, Hutchinson A. 1985. Seasonal cycles of zooplankton from San
687 Francisco Bay. In: Cloern JE, Nichols FH, editors. Temporal Dynamics of an Estuary: San
688 Francisco Bay. Dordrecht: Springer Netherlands. (Developments in Hydrobiology). p. 177–
689 197. [accessed 2020 May 18]. https://doi.org/10.1007/978-94-009-5528-8_11.

690 Anderson RS. 1970. Predator–prey relationships and predation rates for crustacean
691 zooplankters from some lakes in western Canada. Can J Zool. 48(6):1229–1240.
692 doi:10.1139/z70-212.

693 Balcer MD, Korda NL, Dodson SI. 1984. Zooplankton of the Great Lakes: A Guide to the
694 Identification and Ecology of the Common Crustacean Species. Univ of Wisconsin Press.

695 Barros A, Hobbs JA, Willmes M, Parker CM, Bisson M, Fangue NA, Rypel AL, Lewis LS.
696 2022. Spatial Heterogeneity in Prey Availability, Feeding Success, and Dietary Selectivity for
697 the Threatened Longfin Smelt. Estuaries and Coasts. doi:10.1007/s12237-021-01024-y.
698 [accessed 2022 Jan 12]. https://doi.org/10.1007/s12237-021-01024-y.

699 Bashevkin SM. 2021. zooper: an R package to download and integrate zooplankton datasets
700 from the Upper San Francisco Estuary. v2.2.0. Zenodo. doi:10.5281/zenodo.4923868.
701 [accessed 2021 Jun 10]. https://zenodo.org/record/4923868.

702 Bashevkin SM, Hartman R, Thomas M, Barros A, Burdi C, Hennessy A, Tempel T, Kayfetz
703 K. 2020. Interagency Ecological Program: Zooplankton abundance in the Upper San
704 Francisco Estuary from 1972-2018, an integration of 5 long-term monitoring programs.
705 Environmental Data Initiative.
706 doi:10.6073/PASTA/0C400C670830E4C8F7FD45C187EFDCB9. [accessed 2020 Jun 10].
707 https://portal.edirepository.org/nis/mapbrowse?packageid=edi.539.1.

708 Bashevkin SM, Hartman R, Thomas M, Barros A, Burdi CE, Hennessy A, Tempel T, Kayfetz
709 K. 2022. Five decades (1972–2020) of zooplankton monitoring in the upper San Francisco
710 Estuary. PLOS ONE. 17(3):e0265402. doi:10.1371/journal.pone.0265402.

711 Bouley P, Kimmerer WJ. 2006. Ecology of a highly abundant, introduced cyclopoid copepod
712 in a temperate estuary. Marine Ecology Progress Series. 324:219–228.
713 doi:10.3354/meps324219.

714 Brown LR, Bauer ML. 2010. Effects of hydrologic infrastructure on flow regimes of
715 California's Central Valley rivers: Implications for fish populations. River Research and
716 Applications. 26(6):751–765. doi:https://doi.org/10.1002/rra.1293.

717 Brown LR, Kimmerer W, Conrad JL, Lesmeister S, Mueller–Solger A. 2016. Food Webs of
718 the Delta, Suisun Bay, and Suisun Marsh: An Update on Current Understanding and
719 Possibilities for Management. San Francisco Estuary and Watershed Science. 14(3).
720 [accessed 2019 Aug 6]. https://escholarship.org/uc/item/4mk5326r.

721 Bürkner P-C. 2017. brms: An R Package for Bayesian Multilevel Models Using Stan. Journal
722 of Statistical Software. 80(1):1–28. doi:10.18637/jss.v080.i01.

723 Bürkner P-C. 2018. Advanced Bayesian Multilevel Modeling with the R Package brms. The
724 R Journal. 10(1):395–411. doi:10.32614/RJ-2018-017.

725 Carpenter SR, Kitchell JF. 1984. Plankton Community Structure and Limnetic Primary
726 Production. The American Naturalist. 124(2):159–172. doi:10.1086/284261.

727 Chigbu P, Sibley TH. 1998a. Predation by longfin smelt (Spirinchus thaleichthys) on the
728 mysid Neomysis mercedis in Lake Washington. Freshwater Biology. 40(2):295–304.
729 doi:10.1046/j.1365-2427.1998.00354.x.

730 Chigbu P, Sibley TH. 1998b. Feeding ecology of longfin smelt (Spirinchus thaleichthys
731 Ayres) in Lake Washington. Fisheries Research. 38(2):109–119. doi:10.1016/S0165-
732 7836(98)00156-8.

733 Colombano DD, Manfree AD, O□Rear TA, Durand JR, Moyle PB. 2020. Estuarine-
734 terrestrial habitat gradients enhance nursery function for resident and transient fishes in the
735 San Francisco Estuary. Marine Ecology Progress Series. 637:141–157.
736 doi:10.3354/meps13238.

737 Corline NJ, Peek RA, Montgomery J, Katz JVE, Jeffres CA. 2021. Understanding
738 community assembly rules in managed floodplain food webs. Ecosphere. 12(2):e03330.
739 doi:https://doi.org/10.1002/ecs2.3330.

740 Craddock DR, Blahm TH, Parente WD. 1976. Occurrence and Utilization of Zooplankton by
741 Juvenile Chinook Salmon in the Lower Columbia River. Transactions of the American
742 Fisheries Society. 105(1):72–76. doi:10.1577/1548-8659(1976)105<72:OAUOZB>2.0.CO;2.

743 Cushing DH. 1969. The Regularity of the Spawning Season of Some Fishes. ICES Journal of
744 Marine Science. 33(1):81–92. doi:10.1093/icesjms/33.1.81.

745 Cushing DH. 1990. Plankton Production and Year-class Strength in Fish Populations: an
746 Update of the Match/Mismatch Hypothesis. In: Blaxter JHS, Southward AJ, editors.
747 Advances in Marine Biology. Vol. 26. Academic Press. p. 249–293. [accessed 2020 Jul 6].
748 http://www.sciencedirect.com/science/article/pii/S0065288108602023.

749 DeMott WR, Kerfoot WC. 1982. Competition Among Cladocerans: Nature of the Interaction
750 Between Bosmina and Daphnia. Ecology. 63(6):1949–1966. doi:10.2307/1940132.

751 Dodson SI, Grishanin AndreyK, Gross K, Wyngaard GA. 2003. Morphological analysis of
752 some cryptic species in the *Acanthocyclops vernalis* species complex from North America.
753 Hydrobiologia. 500(1):131–143. doi:10.1023/A:1024678018090.

754 Drenner RW, Vinyard GL, O'Brien WJ, Triplett JR, Wagner J. 1981. The Zooplankton
755 Community of Lacygne Lake: A Cooling Pond in Kansas. The Southwestern Naturalist.
756 26(3):243–249. doi:10.2307/3670904.

757 Durant JM, Hjermann DØ, Ottersen G, Stenseth NC. 2007. Climate and the match or
758 mismatch between predator requirements and resource availability. Climate Research.
759 33(3):271–283. doi:10.3354/cr033271.

760 Edwards M, Richardson AJ. 2004. Impact of climate change on marine pelagic phenology
761 and trophic mismatch. Nature. 430(7002):881–884. doi:10.1038/nature02808.

762 Enright C, Culberson SD. 2009. Salinity Trends, Variability, and Control in the Northern
763 Reach of the San Francisco Estuary. San Francisco Estuary and Watershed Science. 7(2).
764 doi:10.15447/sfews.2009v7iss2art3. [accessed 2021 Nov 12].
765 https://escholarship.org/uc/item/0d52737t.

766 Enríquez-García C, Nandini S, Sarma SSS. 2013. Feeding behaviour of *Acanthocyclops*
767 *americanus* (Marsh) (Copepoda: Cyclopoida). Journal of Natural History. 47(5–12):853–862.
768 doi:10.1080/00222933.2012.747637.

769 Evans MS, Stewart JA. 1977. Epibenthic and benthic microcrustaceans (copepods,
770 cladocerans, ostracods) from a nearshore area in southeastern Lake Michigan1. Limnology
771 and Oceanography. 22(6):1059–1066. doi:10.4319/lo.1977.22.6.1059.

772 Feyrer F, Nobriga ML, Sommer TR. 2007. Multidecadal trends for three declining fish
773 species: habitat patterns and mechanisms in the San Francisco Estuary, California, USA. Can
774 J Fish Aquat Sci. 64(4):723–734. doi:10.1139/f07-048.

775 Gliwicz ZM, Stibor H. 1993. Egg predation by copepods in *Daphnia* brood cavities.
776 Oecologia. 95(2):295–298. doi:10.1007/BF00323503.

777 Goertler P, Jones K, Cordell J, Schreier B, Sommer T. 2018. Effects of Extreme Hydrologic
778 Regimes on Juvenile Chinook Salmon Prey Resources and Diet Composition in a Large
779 River Floodplain. Transactions of the American Fisheries Society. 147(2):287–299.
780 doi:10.1002/tafs.10028.

781 Gräler B, Pebesma E, Heuvelink G. 2016. Spatio-temporal interpolation using gstat. RFID
782 Journal. 8(1):204–218.

783 Grimaldo L, Feyrer F, Burns J, Maniscalco D. 2017. Sampling Uncharted Waters: Examining
784 Rearing Habitat of Larval Longfin Smelt (*Spirinchus thaleichthys*) in the Upper San
785 Francisco Estuary. Estuaries and Coasts. 40(6):1771–1784. doi:10.1007/s12237-017-0255-9.

786 Hammock BG, Moose SP, Solis SS, Goharian E, Teh SJ. 2019. Hydrodynamic Modeling
787 Coupled with Long-term Field Data Provide Evidence for Suppression of Phytoplankton by
788 Invasive Clams and Freshwater Exports in the San Francisco Estuary. Environmental
789 Management. 63(6):703–717. doi:10.1007/s00267-019-01159-6.

790 Hart RC. 2004. Cladoceran Periodicity Patterns in Relation to Selected Environmental
791 Factors in Two Cascading Warm-Water Reservoirs Over a Decade. Hydrobiologia.
792 526(1):99–117. doi:10.1023/B:HYDR.0000041610.56021.63.

793 Hennessy A. 2018. Zooplankton Monitoring 2017. Interagency Ecological Program
794 Newsletter. 32(1):21–32.

795 Herbold B, Carlson SM, Henery R, Johnson RC, Mantua N, McClure M, Moyle PB, Sommer
796 T. 2018. Managing for Salmon Resilience in California's Variable and Changing Climate.
797 San Francisco Estuary and Watershed Science. 16(2). doi:10.15447/sfews.2018v16iss2art3.
798 [accessed 2022 Jan 12]. https://escholarship.org/uc/item/8rb3z3nj.

799 Hobbs JA, Bennett WA, Burton JE. 2006. Assessing nursery habitat quality for native smelts
800 (Osmeridae) in the low-salinity zone of the San Francisco estuary. Journal of Fish Biology.
801 69(3):907–922. doi:10.1111/j.1095-8649.2006.01176.x.

802 Holm JChr, Møller D. 1984. Growth and prey selection by Atlantic salmon yearlings reared
803 on live freshwater zooplankton. Aquaculture. 43(4):401–412. doi:10.1016/0044-
804 8486(84)90248-5.

805 Holmes AE, Kimmerer WJ. 2022. Phytoplankton prey of an abundant estuarine copepod
806 identified in situ using DNA metabarcoding. Journal of Plankton Research. 44(2):316–332.
807 doi:10.1093/plankt/fbac002.

808 Hunter JR. 1981. Feeding Ecology and predation of marine fish larvae. In: Lasker R, editor.
809 Marine Fish Larvae: Morphology, Ecology, and Relation to Fisheries. Vol. 1. Seattle:
810 University of Washington Press. p. 33–77.

811 Hutton PH, Rath JS, Roy SB. 2017. Freshwater flow to the San Francisco Bay-Delta estuary
812 over nine decades (Part 1): Trend evaluation. Hydrological Processes. 31(14):2500–2515.
813 doi:10.1002/hyp.11201.

814 Inpang R. 2008. Annual changes of zooplankton communities of different size fractions in
815 Thale-Noi, Phatthalung Province [M.Sc Thesis]. Prince of Songkla University.

816 Jassby AD. 2005. Phytoplankton Regulation in a Eutrophic Tidal River (San Joaquin River,
817 California). San Francisco Estuary and Watershed Science. 3(1).
818 doi:10.15447/sfews.2005v3iss1art5. [accessed 2021 Sep 2].
819 https://escholarship.org/uc/item/9jb2t96d.

820 Jassby AD, Cloern JE, Cole BE. 2002. Annual primary production: Patterns and mechanisms
821 of change in a nutrient-rich tidal ecosystem. Limnology and Oceanography. 47(3):698–712.
822 doi:10.4319/lo.2002.47.3.0698.

823 Jeffres CA, Holmes EJ, Sommer TR, Katz JVE. 2020. Detrital food web contributes to
824 aquatic ecosystem productivity and rapid salmon growth in a managed floodplain. PLOS
825 ONE. 15(9):e0216019. doi:10.1371/journal.pone.0216019.

826 Jiang X, Li Q, Liang H, Zhao S, Zhang L, Zhao Y, Chen L, Yang W, Xiang X. 2013. Clonal
827 Variation in Growth Plasticity within a *Bosmina longirostris* Population: The Potential for
828 Resistance to Toxic Cyanobacteria. PLOS ONE. 8(9):e73540.
829 doi:10.1371/journal.pone.0073540.

830 Jiang X, Xie J, Xu Y, Zhong W, Zhu X, Zhu C. 2017. Increasing dominance of small
831 zooplankton with toxic cyanobacteria. Freshwater Biology. 62(2):429–443.
832 doi:10.1111/fwb.12877.

833 Jiang X, Yang W, Xiang X, Niu Y, Chen L, Zhang J. 2014. Cyanobacteria alter competitive
834 outcomes between *Daphnia* and *Bosmina* in dependence on environmental conditions.
835 Fundamental and Applied Limnology. 184(1):11–22.

836 Jungbluth MJ, Burns J, Grimaldo L, Slaughter A, Katla A, Kimmerer W. 2021. Feeding
837 habits and novel prey of larval fishes in the northern San Francisco Estuary. Environmental
838 DNA. 3(6):1059–1080. doi:10.1002/edn3.226.

839 Jürgens K, Wickham SA, Rothhaupt KO, Santer B. 1996. Feeding rates of macro- and
840 microzooplankton on heterotrophic nanoflagellates. Limnology and Oceanography.
841 41(8):1833–1839. doi:10.4319/lo.1996.41.8.1833.

842 Kayfetz K, Bashevkin SM, Thomas M, Hartman R, Burdi CE, Hennessy A, Tempel T, Barros
843 A. 2020. Zooplankton Integrated Dataset Metadata Report. IEP Technical Report. 93.

844 Kayfetz K, Kimmerer W. 2017. Abiotic and biotic controls on the copepod *Pseudodiaptomus*
845 *forbesi* in the upper San Francisco Estuary. Marine Ecology Progress Series. 581:85–101.
846 doi:10.3354/meps12294.

847 Kerfoot WC. 1978. Combat between predatory copepods and their prey: *Cyclops*, *Epischura*,
848 and *Bosmina*. Limnology and Oceanography. 23(6):1089–1102.
849 doi:10.4319/lo.1978.23.6.1089.

850 Kimmerer W. 2004. Open Water Processes of the San Francisco Estuary: From Physical
851 Forcing to Biological Responses. San Francisco Estuary and Watershed Science. 2(1).
852 doi:10.15447/sfews.2004v2iss1art1. [accessed 2020 Mar 24].
853 https://escholarship.org/uc/item/9bp499mv.

854 Kimmerer W, Ignoffo TR, Bemowski B, Modéran J, Holmes A, Bergamaschi B. 2018.
855 Zooplankton Dynamics in the Cache Slough Complex of the Upper San Francisco Estuary.
856 San Francisco Estuary and Watershed Science. 16(3). doi:10.15447/sfews.2018v16iss3art4.
857 [accessed 2020 May 21]. https://escholarship.org/uc/item/63k1z819.

858 Kimmerer WJ. 2002. Physical, biological, and management responses to variable freshwater
859 flow into the San Francisco Estuary. Estuaries. 25(6):1275–1290. doi:10.1007/BF02692224.

860 Kimmerer WJ, Burau JR, Bennett WA. 2002. Persistence of tidally-oriented vertical
861 migration by zooplankton in a temperate estuary. Estuaries. 25(3):359–371.
862 doi:10.1007/BF02695979.

863 Kimmerer WJ, Ignoffo TR, Slaughter AM, Gould AL. 2014. Food-limited reproduction and
864 growth of three copepod species in the low-salinity zone of the San Francisco Estuary. J
865 Plankton Res. 36(3):722–735. doi:10.1093/plankt/fbt128.

866 Kratina P, Nally RM, Kimmerer WJ, Thomson JR, Winder M. 2014. Human-induced biotic
867 invasions and changes in plankton interaction networks. Journal of Applied Ecology.
868 51(4):1066–1074. doi:10.1111/1365-2664.12266.

869 Kratina P, Winder M. 2015. Biotic invasions can alter nutritional composition of zooplankton
870 communities. Oikos. 124(10):1337–1345. doi:10.1111/oik.02240.

871 Lenoch LK, Stumpner PR, Burau JR, Loken LC, Sadro S. 2021. Dispersion and Stratification
872 Dynamics in the Upper Sacramento River Deep Water Ship Channel. San Francisco Estuary
873 and Watershed Science. 19(4). doi:10.15447/sfews.2021v19iss4art5. [accessed 2021 Dec 16].
874 https://escholarship.org/uc/item/6741j5k3.

875 Lojkovic Burris ZP, Baxter RD, Burdi CE. 2022. Larval and juvenile Longfin Smelt diets as
876 a function of fish size and prey density in the San Francisco Estuary. California Fish and
877 Wildlife Journal. 108(2). doi:10.51492/cfwj.108.11. [accessed 2022 Jul 1].
878 https://wildlife.ca.gov/Publications/Journal/Issues/volume-108-issue-2-larval-and-juvenile-
879 longfin-smelt-diets-as-a-function-of-fish-size-and-prey-density-in-the-san-francisco-estuary.

880 Lucas LV, Cloern JE, Thompson JK, Stacey MT, Koseff JR. 2016. Bivalve Grazing Can
881 Shape Phytoplankton Communities. Frontiers in Marine Science. 3:14.
882 doi:10.3389/fmars.2016.00014.

883 Matveev VF, Balseiro EG. 1990. Contrasting responses of two cladocerans to changes in the
884 nutritional value of nannoplankton. Freshwater Biology. 23(2):197–204.

885 McElreath R. 2015. Statistical rethinking: A Bayesian course with examples in R and Stan.
886 Boca Raton, FL: CRC Press.

887 Merz JE, Bergman PS, Simonis JL, Delaney D, Pierson J, Anders P. 2016. Long-Term
888 Seasonal Trends in the Prey Community of Delta Smelt (*Hypomesus transpacificus*) Within
889 the Sacramento-San Joaquin Delta, California. Estuaries and Coasts. 39(5):1526–1536.
890 doi:10.1007/s12237-016-0097-x.

891 Miracle MR, Alekseev V, Monchenko V, Sentandreu V, Vicente E. 2013. Molecular-genetic-
892 based contribution to the taxonomy of the *Acanthocyclops robustus* group. Journal of Natural
893 History. 47(5–12):863–888. doi:10.1080/00222933.2012.744432.

894 Moyle PB. 2002. Inland Fishes of California: Revised and Expanded. University of
895 California Press.

896 Moyle PB, Brown LR, Durand JR, Hobbs JA. 2016. Delta Smelt: life history and decline of a
897 once-abundant species in the San Francisco Estuary. San Francisco Estuary and Watershed
898 Science. 14(2). doi:10.15447/sfews.2016v14iss2art6. [accessed 2019 Aug 6].
899 https://escholarship.org/uc/item/09k9f76s.

900 Moyle PB, Lund JR, Bennett WA, Fleenor WE. 2010. Habitat Variability and Complexity in
901 the Upper San Francisco Estuary. San Francisco Estuary and Watershed Science. 8(3).
902 doi:https://doi.org/10.15447/sfews.2010v8iss3art1. [accessed 2021 Feb 2].
903 https://escholarship.org/uc/item/0kf0d32x.

904 Onandia G, Dias JD, Miracle MR. 2015. Zooplankton grazing on natural algae and bacteria
905 under hypertrophic conditions. Limnetica. 34(2):541–560.

906 Orsi JJ, Mecum WL. 1986. Zooplankton distribution and abundance in the Sacramento-San
907 Joaquin delta in relation to certain environmental factors. Estuaries. 9(4):326–339.
908 doi:10.2307/1351412.

909 Orsi JJ, Ohtsuka S. 1999. Introduction of the Asian copepods *Acartiella sinensis*, *Tortanus*
910 *dextrilobatus* (Copepoda: Calanoida), and *Limnoithona tetraspina* (Copepoda: Cyclopoida) to
911 the San Francisco Estuary, California, USA. Plankton Biology and Ecology. 46(2):128–131.

912 Orsi JJ, Walter TE. 1991. *Pseudodiaptomus forbesi* and *P. marinus* (Copepoda Calanoida),
913 the latest copepod immigrants to California's Sacramento-San Joaquin Estuary. In: Uye SI,
914 Nishida S, Ho J-S, editors. Proc. Fourth Internl. Conf. on Copepoda. Hiroshima: Bull.
915 Plankton Soc. Jpn. p. 553–562.

916 Pebesma EJ. 2004. Multivariable geostatistics in S: the gstat package. Computers &
917 Geosciences. 30(7):683–691. doi:10.1016/j.cageo.2004.03.012.

918 Phillis CC, Sturrock AM, Johnson RC, Weber PK. 2018. Endangered winter-run Chinook
919 salmon rely on diverse rearing habitats in a highly altered landscape. Biological
920 Conservation. 217:358–362. doi:10.1016/j.biocon.2017.10.023.

921 Piasecki WG. 2000. Attacks of cyclopoid *Acanthocyclops robustus* [Sars] on newly hatched
922 cyprinids. Electronic Journal of Polish Agricultural Universities Series Fisheries. 1(03).
923 [accessed 2021 Sep 3]. https://www.infona.pl//resource/bwmeta1.element.agro-article-
924 c69d1cf5-d408-436f-9b5e-810f38f00c59.

925 Roegner C, Bottom D, Baptista A, Campbell L, Goertler P, Hinton S, McNatt R, Simenstad
926 C, Teel D, Fresh K. 2015. Salmon Habitat Use of Tidal-fluvial Habitats of the Columbia
927 River Estuary, 2010-2013. Final Report. Report of research by NOAA Fisheries, Northwest
928 Fisheries Science Center to US Army Corps of Engineers, Portland District.

929 Romare P. 2000. Growth of larval and juvenile perch: the importance of diet and fish density.
930 Journal of Fish Biology. 56(4):876–889. doi:10.1111/j.1095-8649.2000.tb00878.x.

931 Sarma SSS, Miracle MR, Nandini S, Vicente E. 2019. Predation by *Acanthocyclops*
932 *americanus* (Copepoda: Cyclopoida) in the hypertrophic shallow waterbody, Lake Albufera
933 (Spain): field and laboratory observations. Hydrobiologia. 829(1):5–17. doi:10.1007/s10750-
934 018-3546-7.

935 Shen C-J, Lee F. 1963. The estuarine copepoda of Chiekong and Zaikong rivers, Kwangtung
936 Province China. Acta Zool Sin. 15:571–596.

937 Slater SB, Baxter RD. 2014. Diet, prey selection, and body condition of age-0 Delta Smelt,
938 *Hypomesus transpacificus*, in the upper San Francisco Estuary. San Francisco Estuary and
939 Watershed Science. 12(3). [accessed 2020 Jan 24]. https://escholarship.org/uc/item/52k878sb.

940 Slater SB, Schultz A, Hammock BG, Hennessy A, Burdi C. 2019. Patterns of Zooplankton
941 Consumption by Juvenile and Adult Delta Smelt (*Hypomesus transpacifus*). In: Schultz A,
942 editor. Directed Outflow Project Technical Report 1. Sacramento, CA: U. S. Bureau of
943 Reclamation,Bay-Delta Office, Mid-Pacific Region.

944 Slaughter AM, Ignoffo TR, Kimmerer W. 2016. Predation impact of *Acartiella sinensis*, an
945 introduced predatory copepod in the San Francisco Estuary, USA. Marine Ecology Progress
946 Series. 547:47–60. doi:10.3354/meps11640.

947 Sogard SM. 1997. Size-Selective Mortality in the Juvenile Stage of Teleost Fishes: A
948 Review. Bulletin of Marine Science. 60(3):1129–1157.

949 Sommer T, Mejia F. 2013. A Place to Call Home: A Synthesis of Delta Smelt Habitat in the
950 Upper San Francisco Estuary. San Francisco Estuary and Watershed Science. 11(2).
951 doi:10.15447/sfews.2013v11iss2art4. [accessed 2021 May 13].
952 https://escholarship.org/uc/item/32c8t244.

953 Sommer TR, Armor C, Baxter R, Breuer R, Brown L, Chotkowski M, Culberson S, Feyrer F,
954 Gingras M, Herbold B, et al. 2007. The Collapse of Pelagic Fishes in the Upper San
955 Francisco Estuary: El Colapso de los Peces Pelagicos en La Cabecera Del Estuario San
956 Francisco. Fisheries. 32(6):270–277. doi:10.1577/1548-
957 8446(2007)32[270:TCOPFI]2.0.CO;2.

958 Srinui K, Ohtsuka S. 2015. Supplementary Description of Three *Acartiella* Species
959 (Crustacea: Copepoda: Calanoida) from Estuarine Waters in Thailand. Species Diversity.
960 20(2):167–181. doi:10.12782/sd.20.2.167.

961 Stan Development Team. 2021. Stan User's Guide. Version 2.27. [accessed 2020 Oct 14].
962 https://mc-stan.org/docs/2_24/stan-users-guide/index.html.

963 Tan Y, Huang L, Chen Q, Huang X. 2004. Seasonal variation in zooplankton composition
964 and grazing impact on phytoplankton standing stock in the Pearl River Estuary, China.
965 Continental Shelf Research. 24(16):1949–1968. doi:10.1016/j.csr.2004.06.018.

966 Tõnno I, Agasild H, Kõiv T, Freiberg R, Nõges P, Nõges T. 2016. Algal Diet of Small-
967 Bodied Crustacean Zooplankton in a Cyanobacteria-Dominated Eutrophic Lake. PLOS ONE.
968 11(4):e0154526. doi:10.1371/journal.pone.0154526.

969 Vehtari A, Gelman A, Gabry J. 2017. Practical Bayesian model evaluation using leave-one-
970 out cross-validation and WAIC. Stat Comput. 27(5):1413–1432. doi:10.1007/s11222-016-
971 9696-4.

972 Vroom J, Wegen M van der, Martyr-Koller RC, Lucas LV. 2017. What Determines Water
973 Temperature Dynamics in the San Francisco Bay-Delta System? Water Resources Research.
974 53(11):9901–9921. doi:10.1002/2016WR020062.

975 Winder M, Jassby AD. 2011. Shifts in Zooplankton Community Structure: Implications for
976 Food Web Processes in the Upper San Francisco Estuary. Estuaries and Coasts. 34(4):675–
977 690. doi:10.1007/s12237-010-9342-x.

978 Wood SN. 2011. Fast stable restricted maximum likelihood and marginal likelihood
979 estimation of semiparametric generalized linear models. Journal of the Royal Statistical
980 Society: Series B (Statistical Methodology). 73(1):3–36. doi:https://doi.org/10.1111/j.1467-
981 9868.2010.00749.x.

982 York JK, McManus GB, Kimmerer WJ, Slaughter AM, Ignoffo TR. 2014. Trophic Links in
983 the Plankton in the Low Salinity Zone of a Large Temperate Estuary: Top-down Effects of
984 Introduced Copepods. Estuaries and Coasts. 37(3):576–588. doi:10.1007/s12237-013-9698-9.

985 Young MJ, Feyrer F, Stumpner PR, Larwood V, Patton O, Brown LR. 2021. Hydrodynamics
986 drive pelagic communities and food web structure in a tidal environment. International
987 Review of Hydrobiology. 106(2):69–85. doi:https://doi.org/10.1002/iroh.202002063.

988 Zeug SC, Wiesenfeld J, Sellheim K, Brodsky A, Merz JE. 2019. Assessment of Juvenile
989 Chinook Salmon Rearing Habitat Potential Prior to Species Reintroduction. North American
990 Journal of Fisheries Management. 39(4):762–777. doi:10.1002/nafm.10309.

991